Invisible Axion Search Methods

Pierre Sikivie (U of Florida)

Quantum Universe Colloquium

DESY, June 29, 2022

Supported by US Department of Energy grant DE-SC0022148

The Strong CP Problem

$$\mathcal{L}_{\mathrm{QCD}} = \ \dots \ + \ \bar{\theta} \frac{g^2}{32\pi^2} G^a_{\mu\nu} \tilde{G}^{a\mu\nu}$$

with
$$\bar{\theta} = \theta - \arg(m_u\, m_d \ \dots \ m_t)$$
$$= \theta - \arg\det(Y^u\, Y^d)$$

is expected to be of order one, whereas the absence of P and CP violation in the strong interactions requires

$$\bar{\theta} \leq 10^{-10}$$

from upper limit
on the neutron electric
dipole moment

A level pooltable on an inclined floor

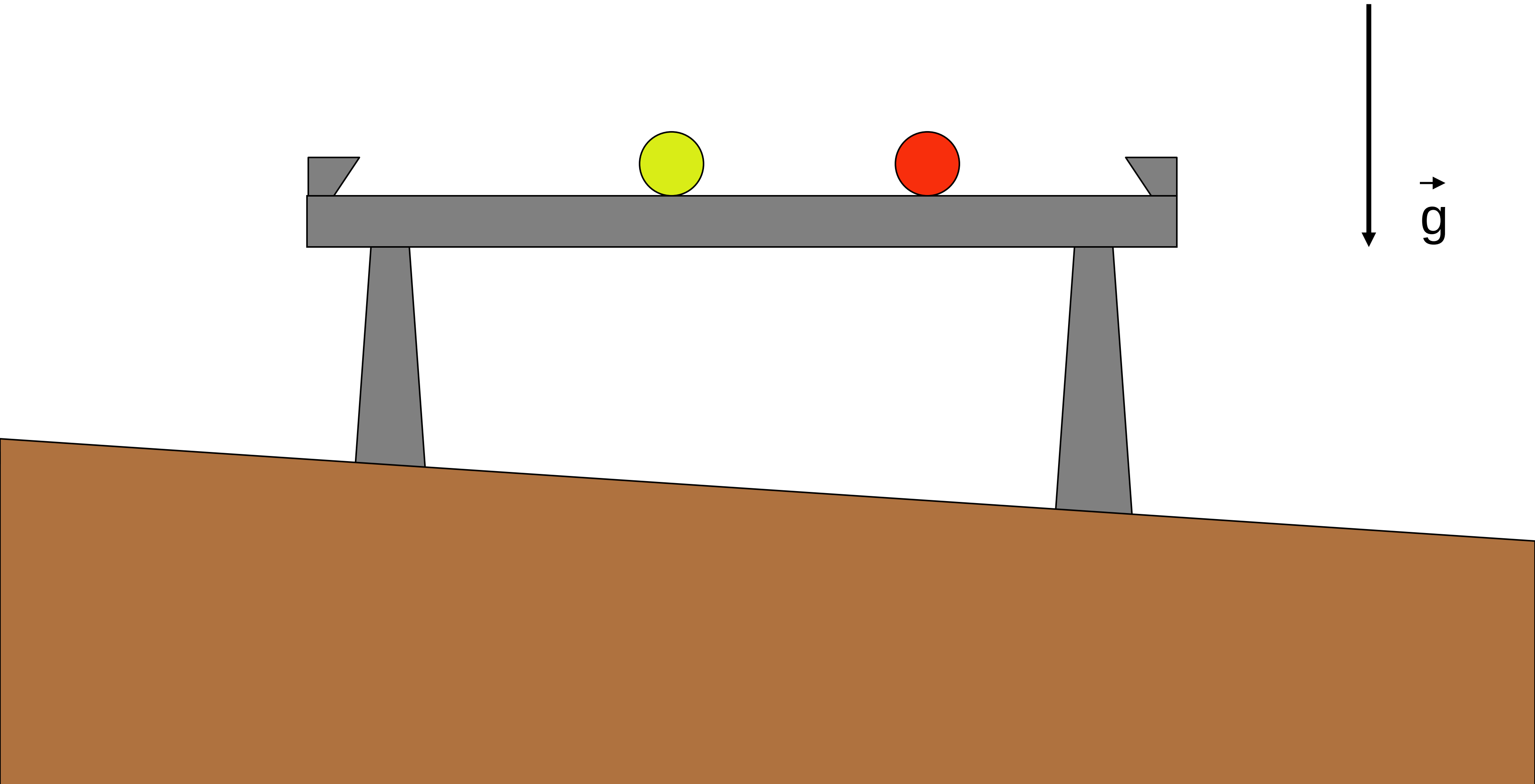

$$U_{PQ}(1)$$

- is a symmetry of the classical action
- is spontaneously broken
- has a color anomaly

Peccei and Quinn, 1977

If a $U_{PQ}(1)$ symmetry is assumed,

$$\mathcal{L} = \ ... \ + \ \frac{a}{f_a}\frac{g^2}{32\pi^2}G^a_{\mu\nu}\tilde{G}^{a\mu\nu} \ + \ \frac{1}{2}\partial_\mu a \partial^\mu a$$

$\bar{\theta} = \dfrac{a}{f_a}$ relaxes to zero,

and a light neutral pseudoscalar particle is predicted: the axion.

Weinberg, Wilczek 1978

A self adjusting pooltable

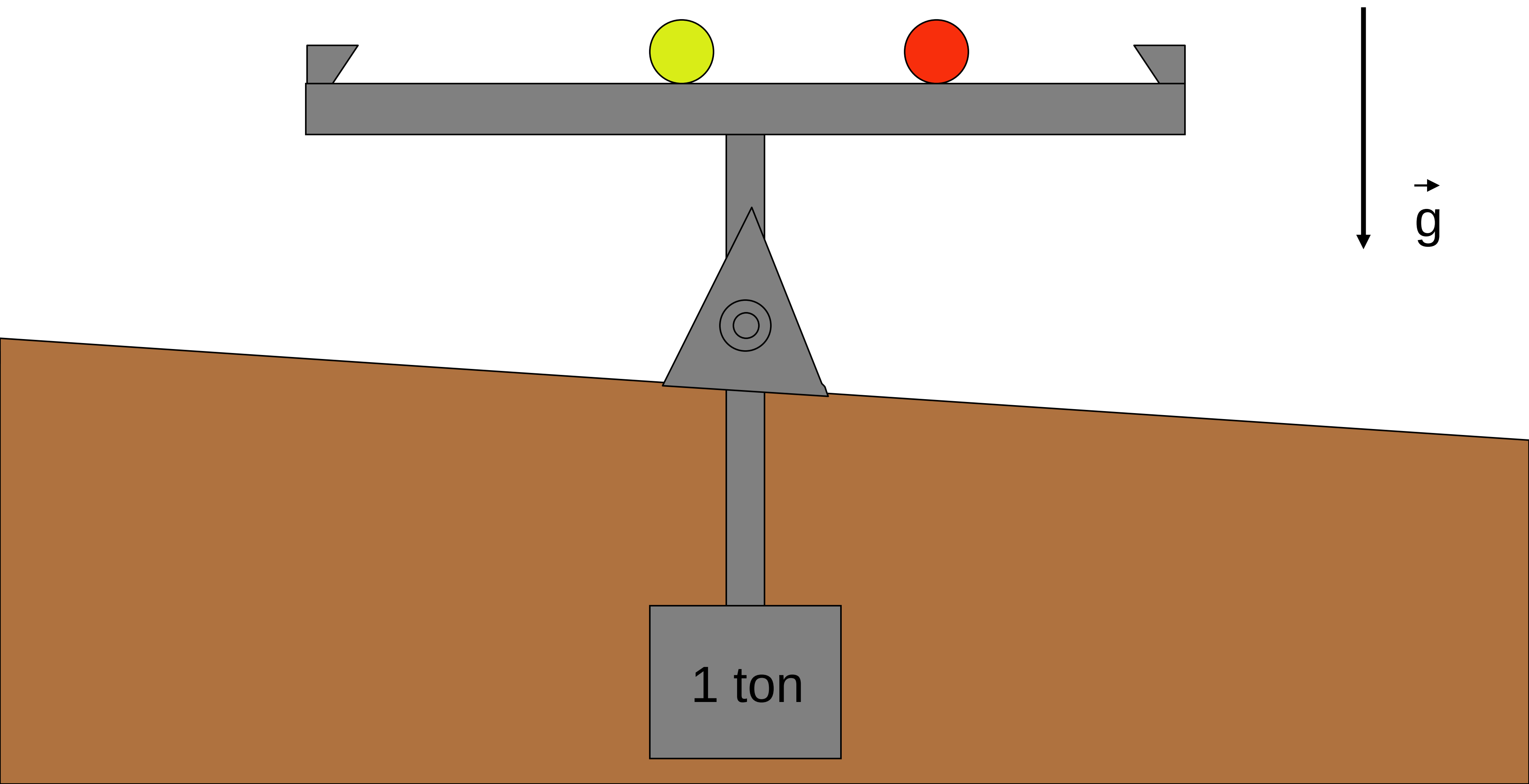

Searching for the pooltable oscillation quantum

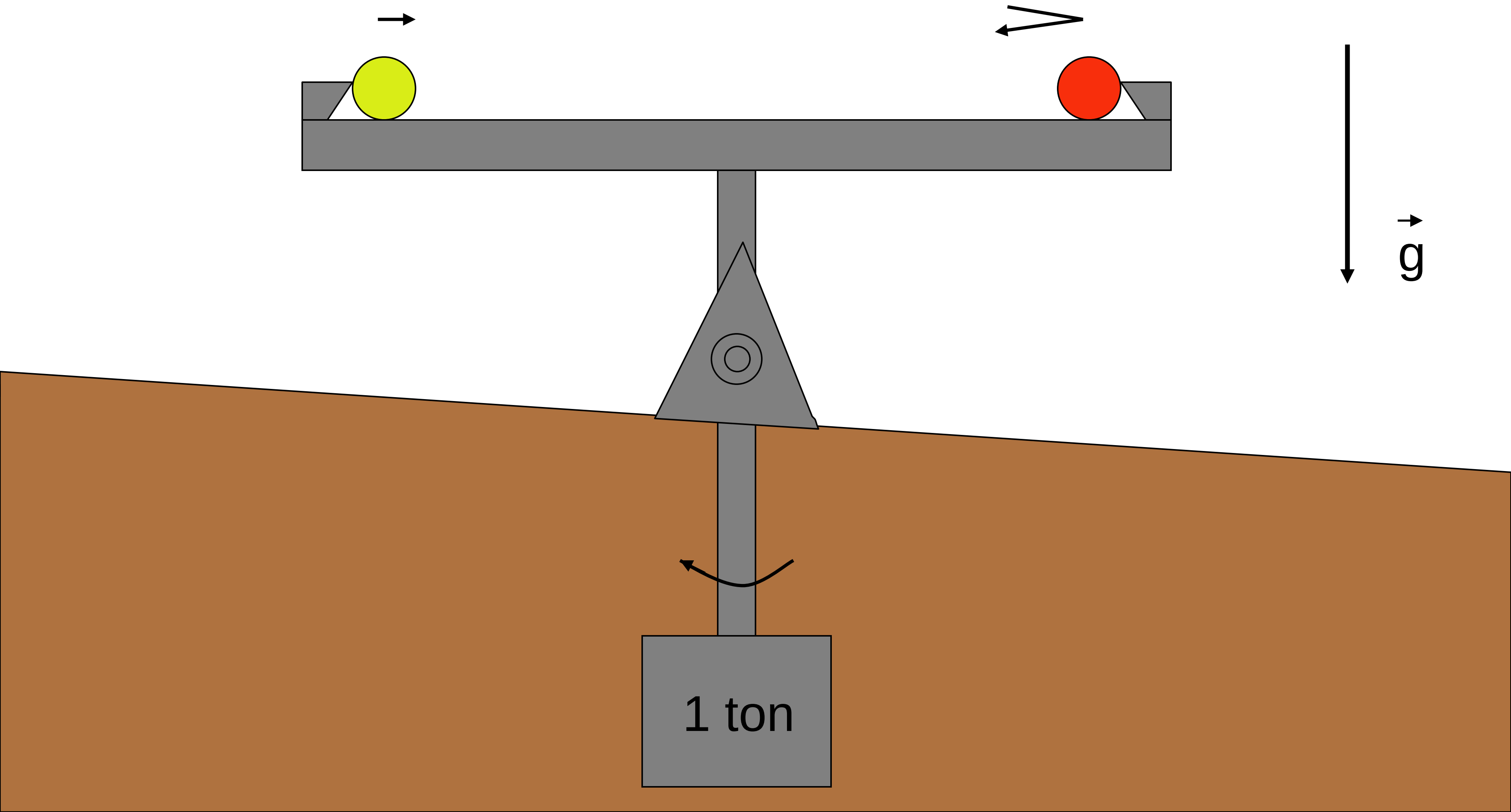

$$m_a \simeq 6\ \mathrm{eV}\ \frac{10^6\ \mathrm{GeV}}{f_a}$$

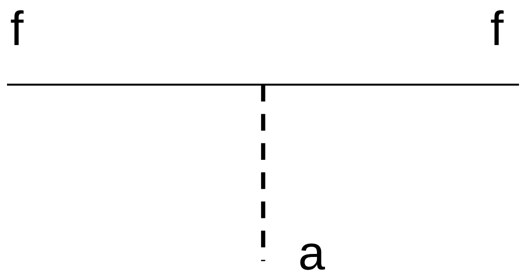

$$\mathcal{L}_{a\bar{f}f} = i g_f \frac{a(x)}{f_a} \bar{f}(x)\gamma^5 f(x)$$

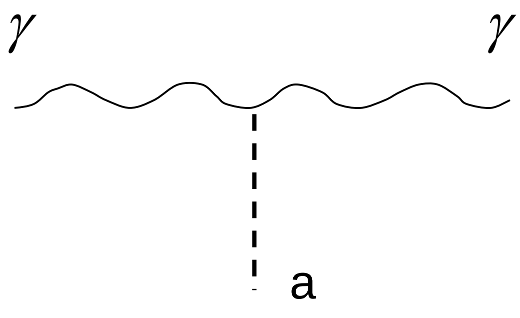

$$\mathcal{L}_{a\gamma\gamma} = -g_\gamma \frac{\alpha}{\pi} \frac{1}{f_a} a(x)\vec{E}(x) \cdot \vec{B}(x)$$

g_γ = 0.97 in KSVZ model

0.36 in DFSZ model

Axions are constrained by

- beam dump experiments
- rare particle decays $(e.g.\ \ K^+ \rightarrow \pi^+\ a)$
- radiative corrections

  $(e.g.\ \ \mathrm{the}\ \mu^-\ \mathrm{anomalous\ magnetic\ moment})$
- the evolution of stars

Axion constraints

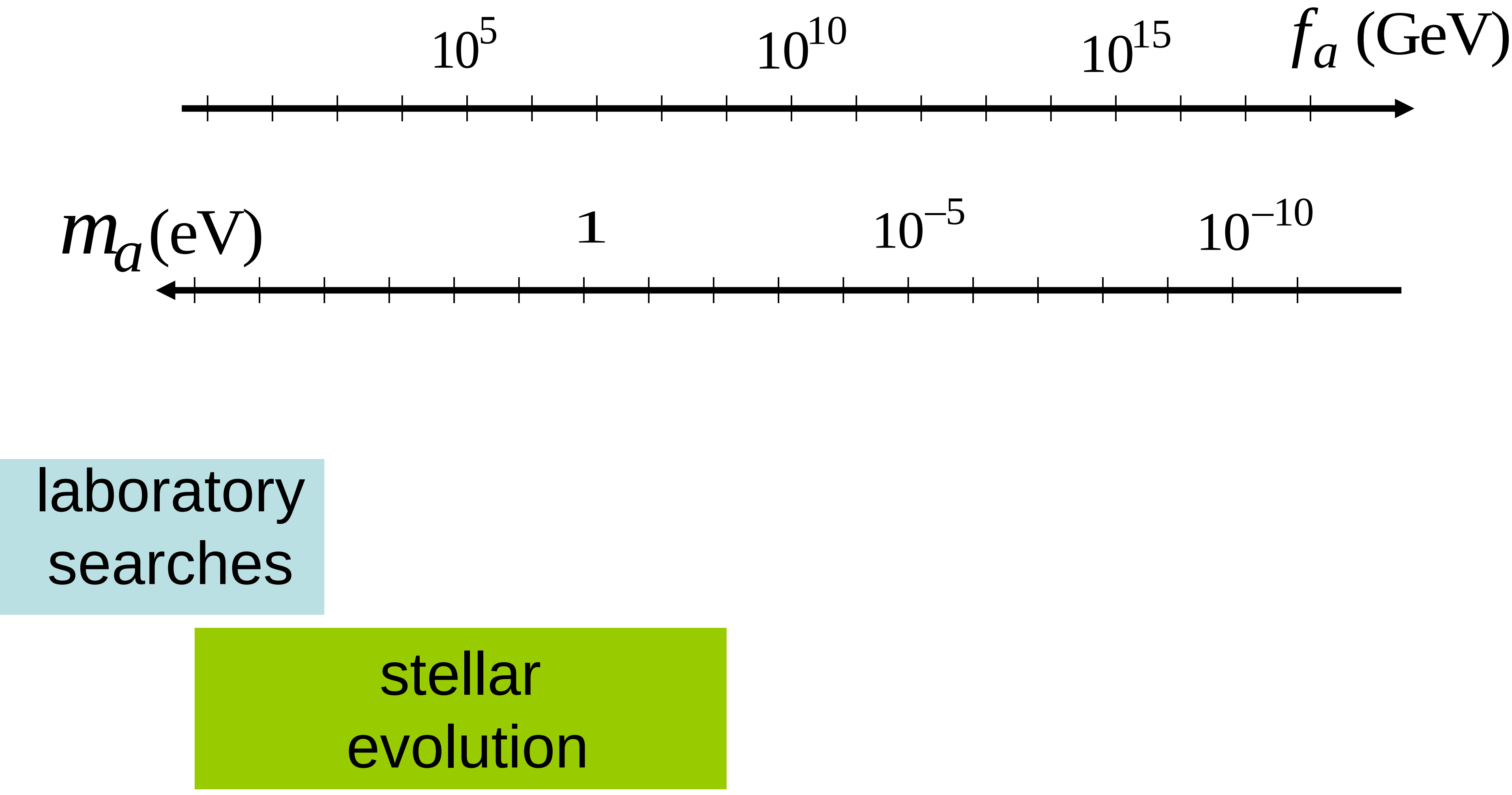

A self adjusting pooltable

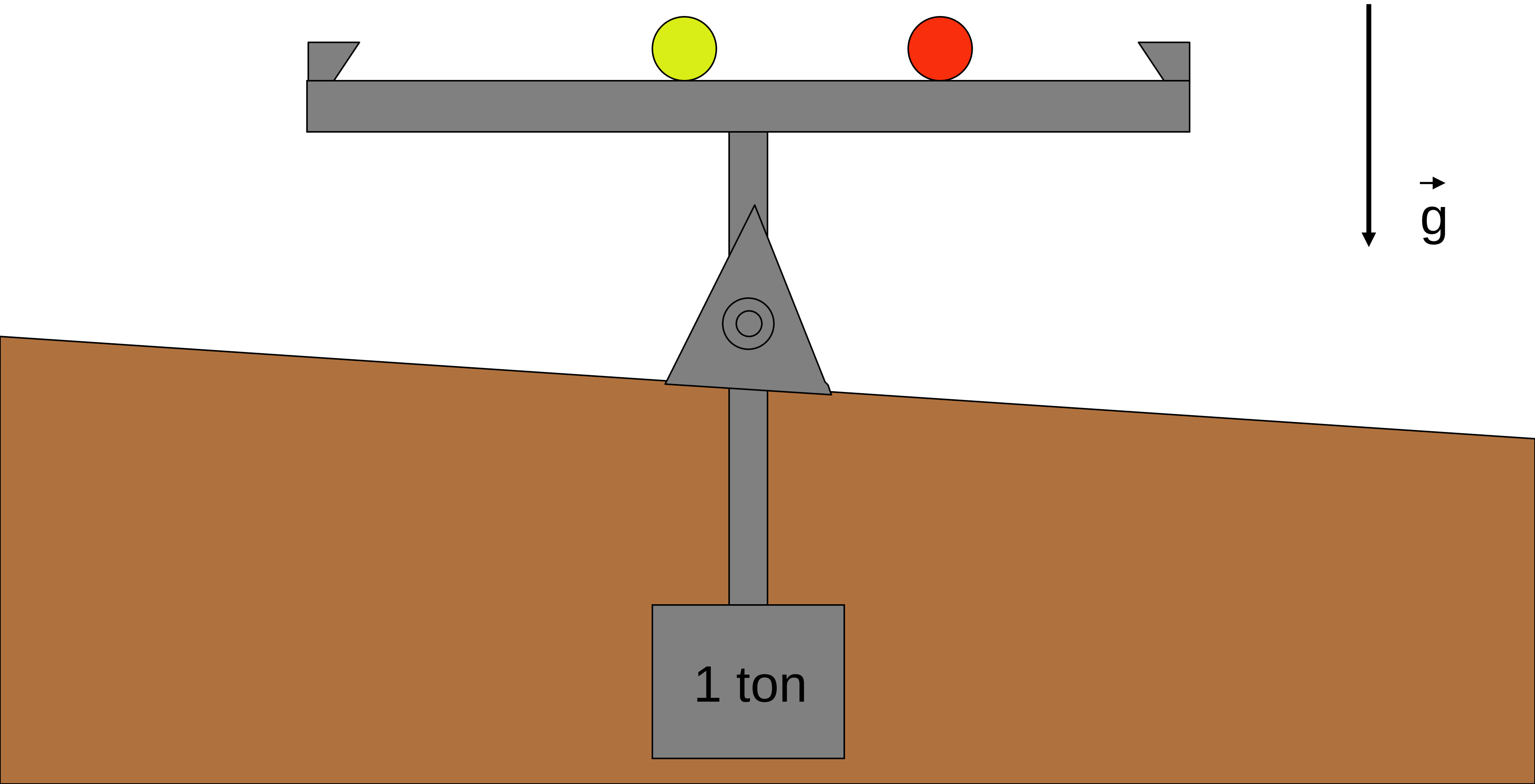

Axion constraints

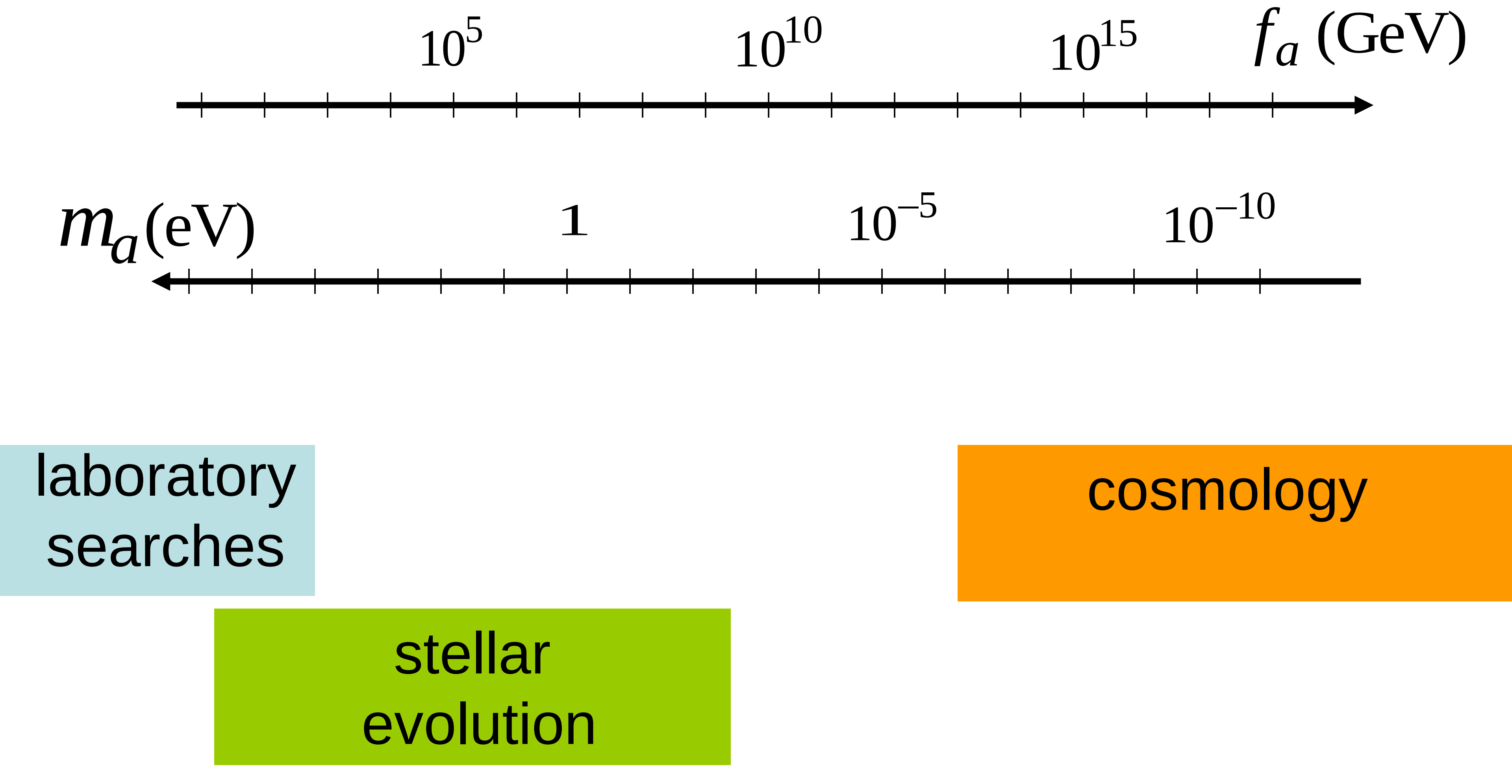

Thermal axions

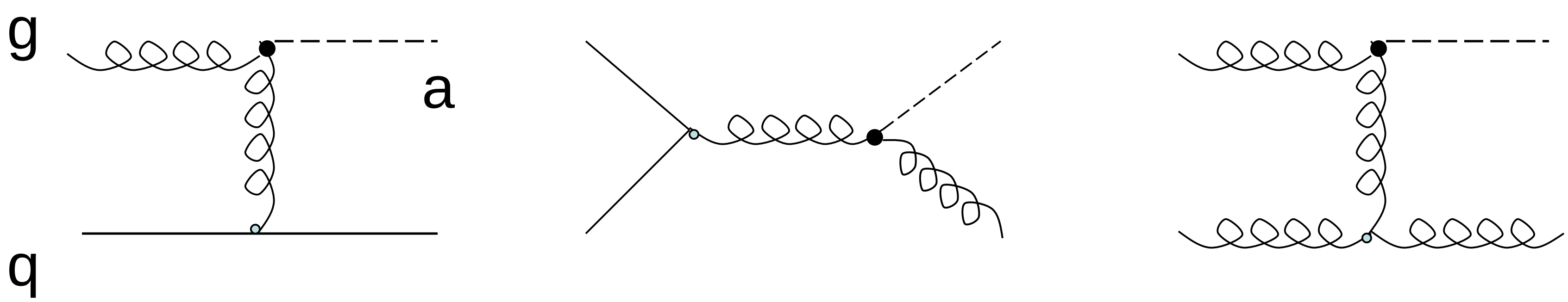

these processes imply an axion decoupling temperature

$$T_D \simeq 3 \times 10^{11}\ \mathrm{GeV} \left(\frac{f_a}{10^{12}\ \mathrm{GeV}} \right)^2$$

thermal axion temperature today:

$$T_a\left(t_0\right) = 0.908\ \mathrm{K} \left(\frac{106.75}{N_\mathrm{D}} \right)^{\frac{1}{3}}$$

N_D = effective number of thermal degrees of freedom at axion decoupling

There are two cosmic axion populations: hot and cold.

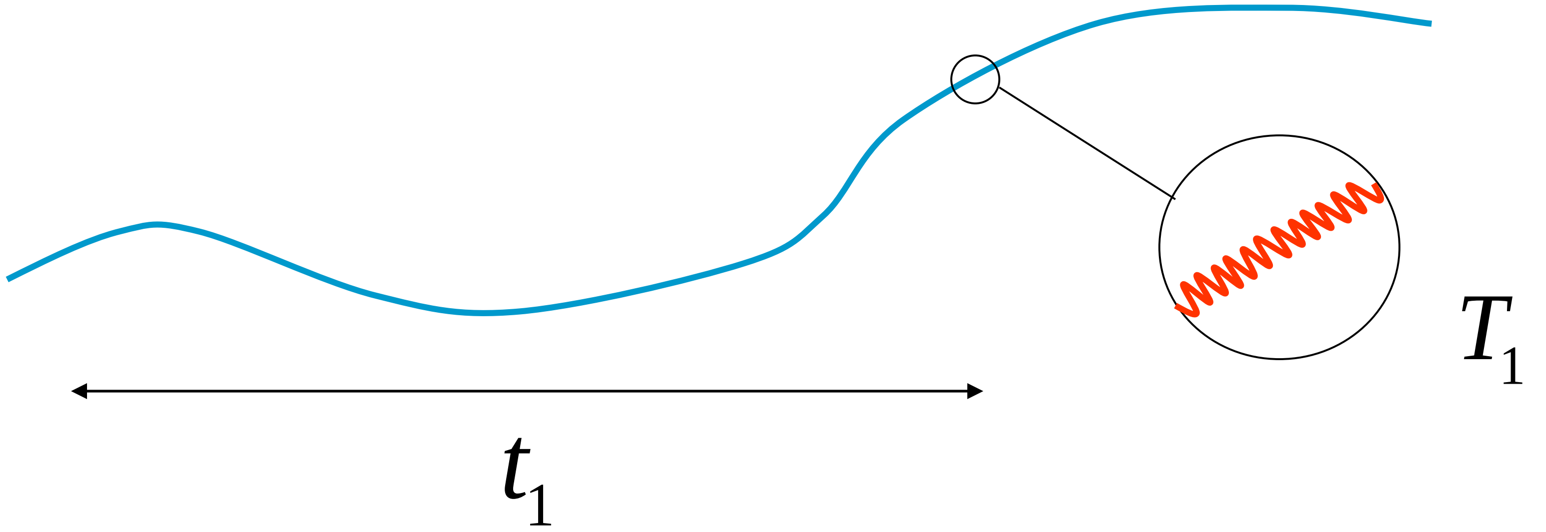

When the axion mass turns on, at QCD time,

$$T_1 \simeq 1 \text{ GeV}$$

$$t_1 \simeq 2 \times 10^{-7} \text{ sec}$$

$$p_a(t_1) \simeq \frac{1}{t_1} \simeq 3 \times 10^{-9} \text{ eV}$$

Effective potential V(T,Φ)

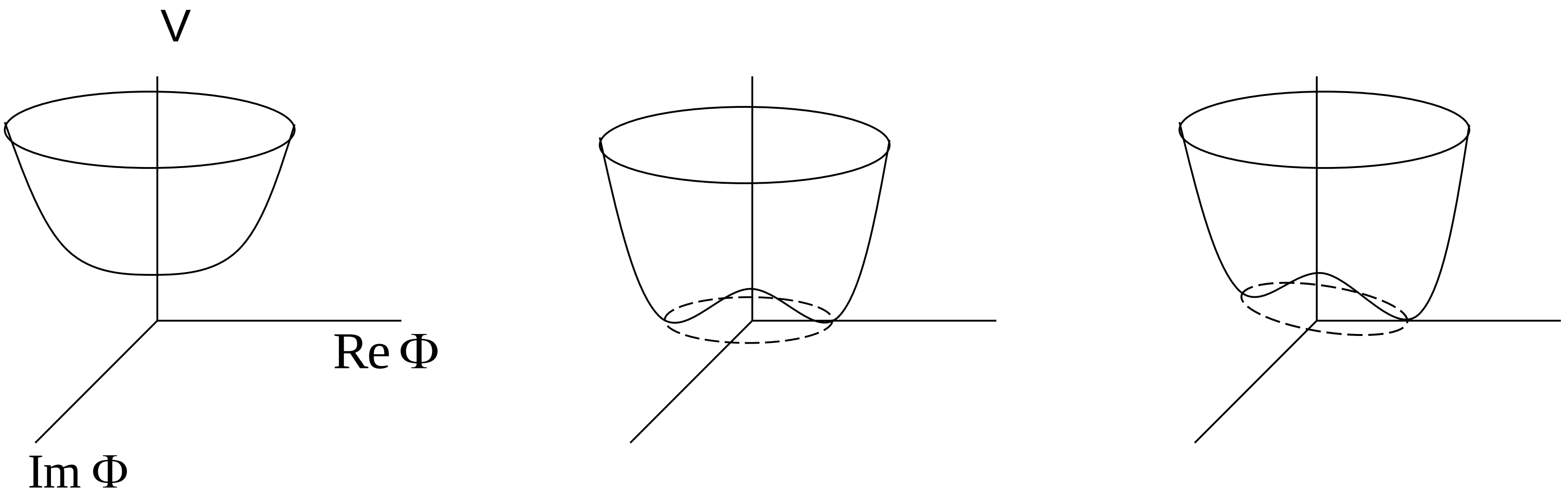

$T > f_a$

$f_a > T > 1\,\mathrm{GeV}$ → axion strings

$1\,\mathrm{GeV} > T$ → axion domain walls

Axion production by vacuum realignment

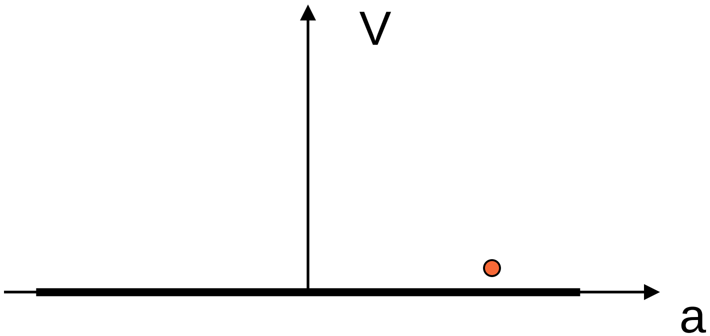

$T \geq 1\,\mathrm{GeV}$

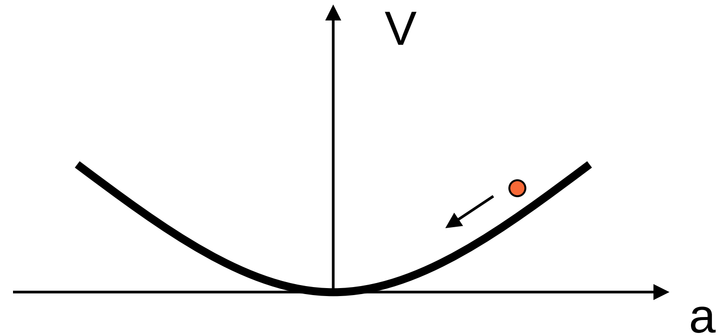

$T \leq 1\,\mathrm{GeV}$

$$n_a(t_1) \simeq \frac{1}{2} m_a(t_1) a(t_1)^2 \simeq \frac{1}{2t_1} f_a^2 \alpha(t_1)^2$$

$$\rho_a(t_0) \simeq m_a n_a(t_1) \left(\frac{R_1}{R_0}\right)^3 \propto m_a^{-\frac{7}{6}}$$

initial misalignment angle

J. Preskill, M. Wise & F. Wilczek, L. Abbott & PS, M. Dine & W. Fischler, 1983

Axion constraints

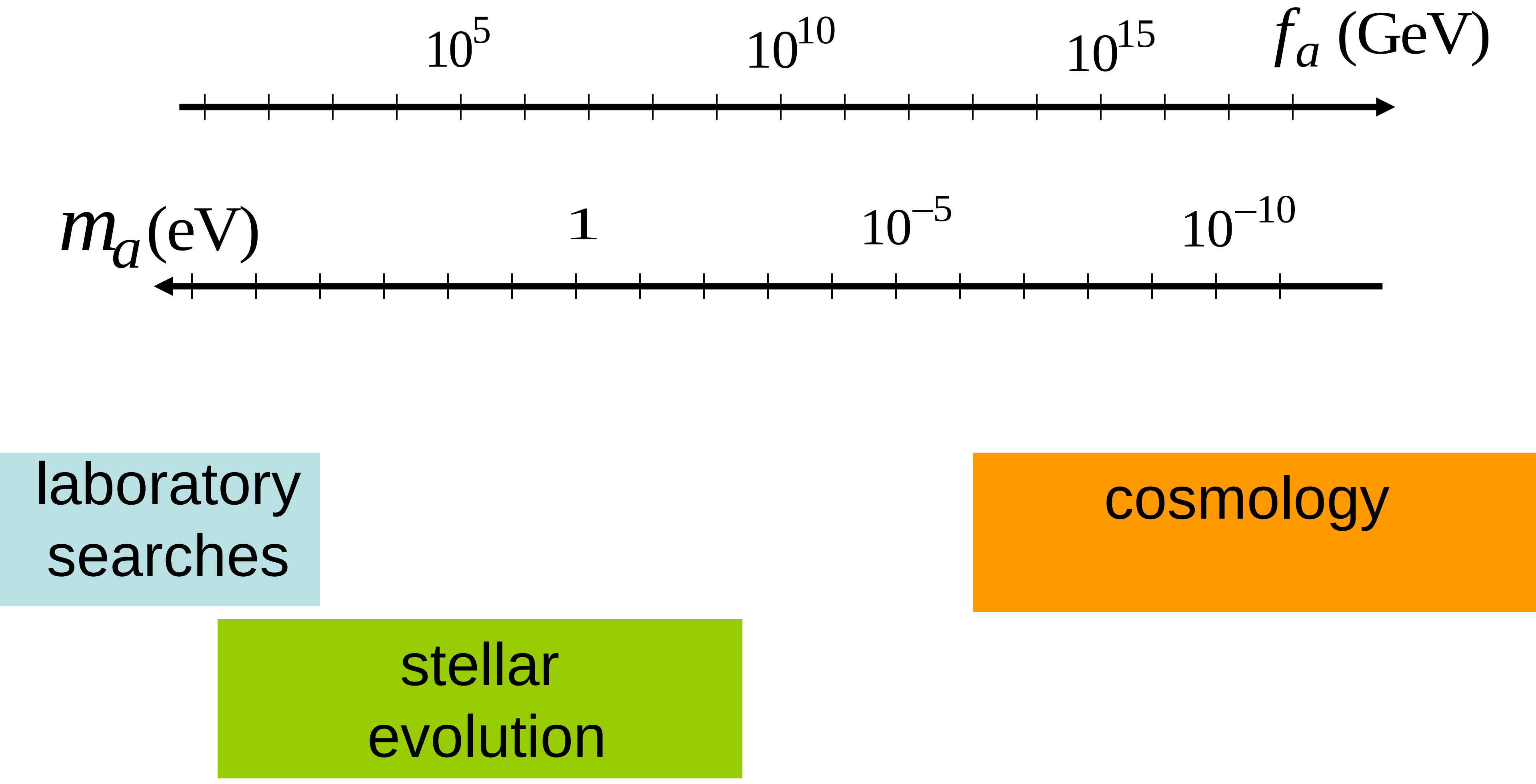

Remaining topics

axion electrodynamics

the cavity haloscope

solar axion searches

shining light through walls

dielectric haloscopes

NMR methods

axion mediated long-range forces

LC circuit

axion echo

The Witten Effect (1979)

When $\theta \neq 0$ magnetic monopoles acquire electric charge

$$q_e = \frac{\alpha}{\pi}\,\theta\, q_m$$

$$q_e = \frac{\alpha}{\pi}(\theta + \frac{a}{f_a})q_m$$ with axion

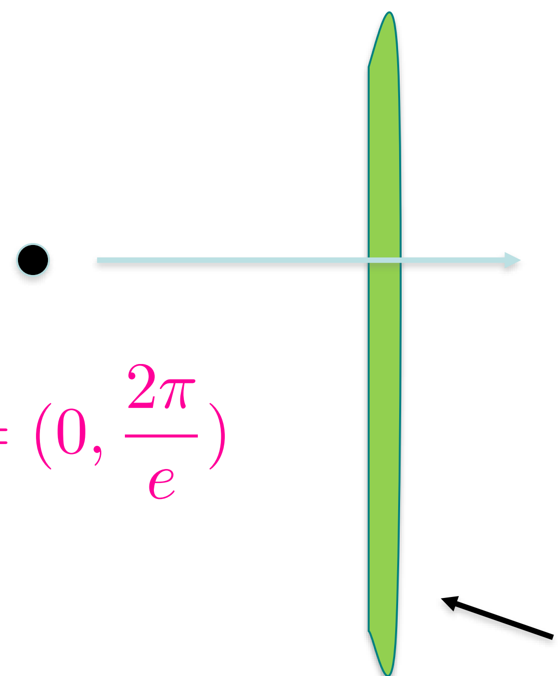

$$(q_e, q_m) = (0, \frac{2\pi}{e})$$

$$\frac{e^2}{4\pi}\frac{1}{\pi}\frac{2\pi}{e}\;2\pi = e$$

The Witten Effect (1979)

When $\theta \neq 0$ magnetic monopoles acquire electric charge

$$q_e = \frac{\alpha}{\pi}\,\theta\; q_m$$

$$q_e = \frac{\alpha}{\pi}(\theta + \frac{a}{f_a})q_m$$

with axion

$$(q_e, q_m) = (0, \frac{2\pi}{e})$$

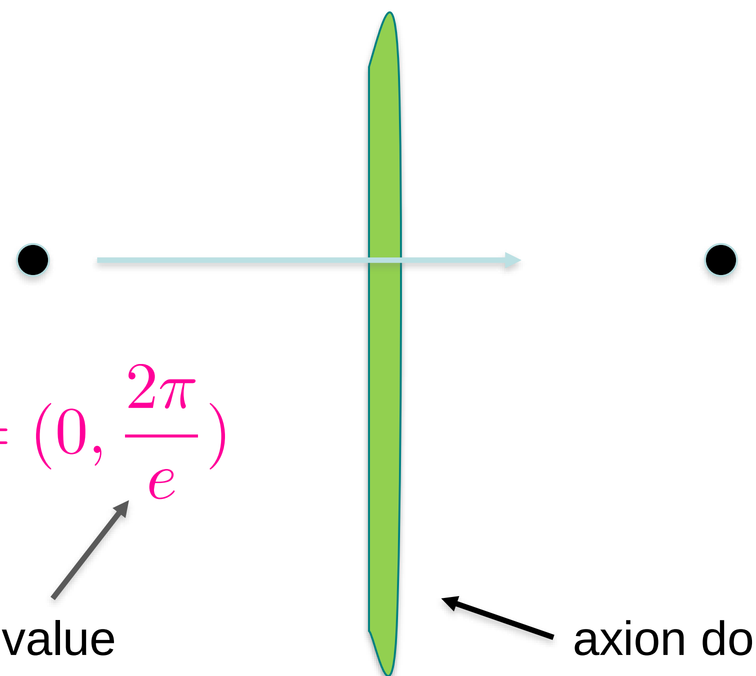

The Witten Effect (1979)

When $\theta \neq 0$ magnetic monopoles acquire electric charge

$$q_e = \frac{\alpha}{\pi}\,\theta\,q_m$$

$$q_e = \frac{\alpha}{\pi}(\theta + \frac{a}{f_a})q_m$$ with axion

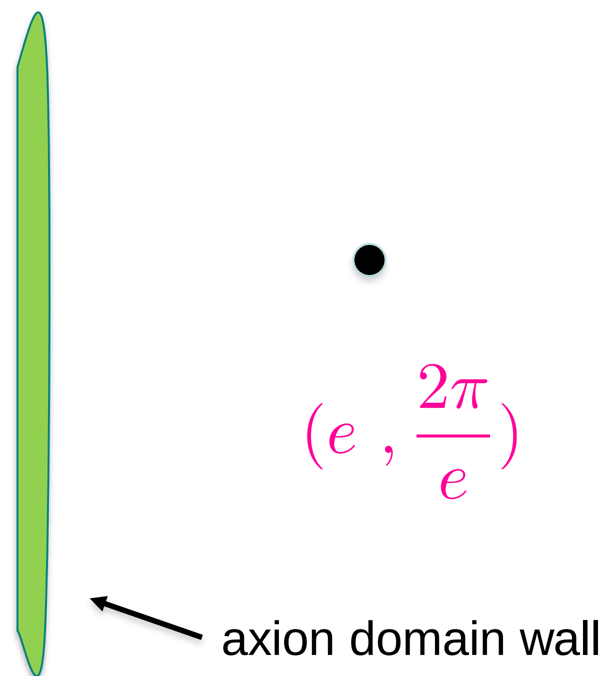

Axion Electrodynamics

$$\mathcal{L} = \frac{1}{2}(\vec{E}(x) \cdot \vec{E}(x) - \vec{B}(x) \cdot \vec{B}(x))$$

$$+\frac{1}{2}(\partial_t a(x)\partial_t a(x) - \vec{\nabla} a(x) \cdot \vec{\nabla} a(x))$$

$$-\frac{1}{2}m_a^2 a(x)^2$$

$$-g_\gamma \frac{\alpha}{\pi}\frac{1}{f_a} a(x)\vec{E}(x) \cdot \vec{B}(x)$$

$$g = g_\gamma \frac{\alpha}{\pi}\frac{1}{f_a}$$

Axion Electrodynamics

PS, 83

$$\vec{\nabla} \cdot (\vec{E} - ga\vec{B}) = \rho_{\rm el}$$

$$g = g_\gamma \frac{\alpha}{\pi} \frac{1}{f_a}$$

$$\vec{\nabla} \times (\vec{B} + ga\vec{E}) - \partial_t(\vec{E} - ga\vec{B}) = \vec{j}_{\rm el}$$

$$\vec{\nabla} \times \vec{E} + \partial_t \vec{B} = 0$$

$$\vec{\nabla} \cdot \vec{B} = 0$$

$$\partial_t^2 a - \nabla^2 a + m_a^2 a = -g\vec{E} \cdot \vec{B}$$

$$\vec{\nabla} \cdot \vec{E} = g\vec{\nabla} a \cdot \vec{B} + ga\vec{\nabla} \cdot \vec{B}$$

Witten Effect

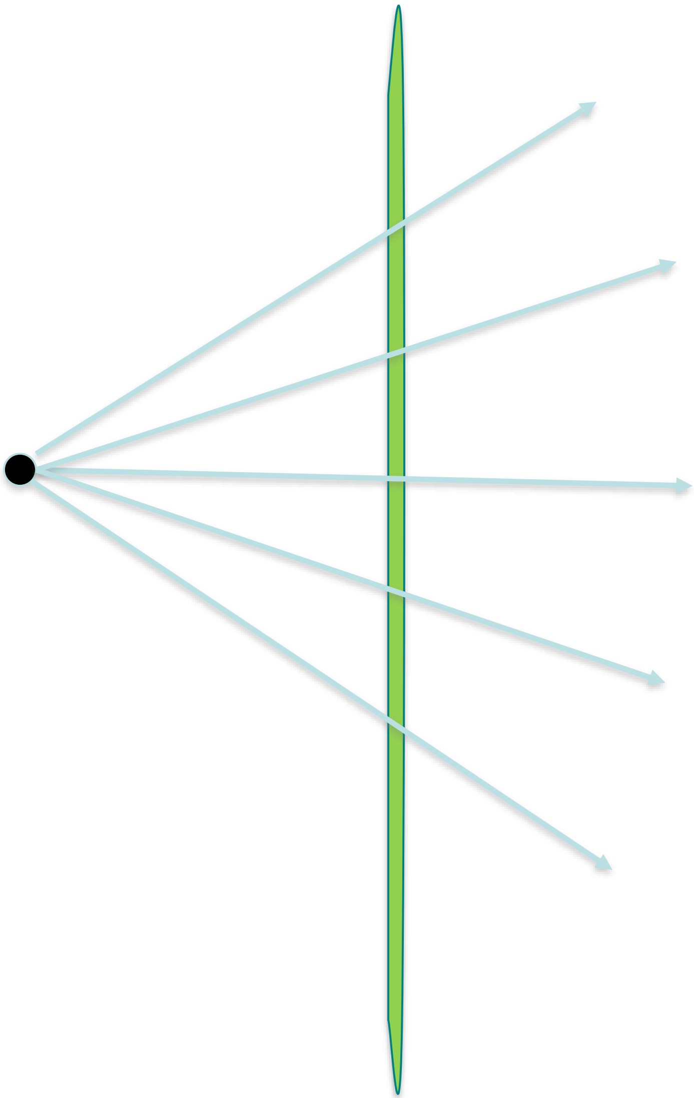

electric charge
surface density

$$\sigma_{\mathrm{el}} = g\Delta a B_{\perp} = 2\alpha B_{\perp}$$

Axion Electrodynamics

$$\vec{\nabla} \cdot (\vec{E} - ga\vec{B}) = \rho_{\mathrm{el}}$$

$$\vec{\nabla} \times (\vec{B} + ga\vec{E}) - \partial_t(\vec{E} - ga\vec{B}) = \vec{j}_{\mathrm{el}}$$

$$\vec{\nabla} \times \vec{E} + \partial_t \vec{B} = 0$$

$$\vec{\nabla} \cdot \vec{B} = 0$$

$$\partial_t^2 a - \nabla^2 a + m_a^2 a = -g\vec{E} \cdot \vec{B}$$

$$\vec{\nabla} \times \vec{B} - \partial_t \vec{E} = -g\vec{B}\partial_t a + g\vec{E} \times \vec{\nabla} a$$

In background electric and magnetic fields
the axion field is a source of electromagnetic radiation

$$\partial_t^2 \vec{A} - \nabla^2 \vec{A} = g(\vec{E}_0 \times \vec{\nabla} a - \vec{B}_0 \partial_t a)$$

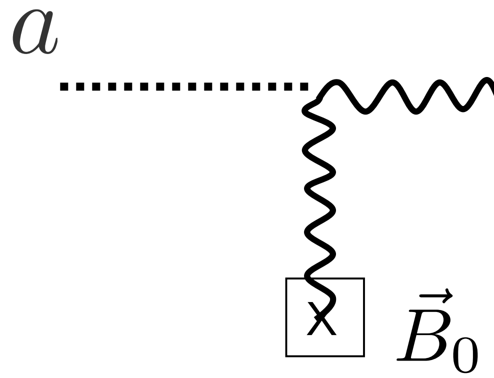

Axions convert to photons in a magnetic field and vice-versa

$$\partial_t^2 a - \nabla^2 a + m_a^2 a = -g\vec{B}_0 \cdot \vec{E}$$

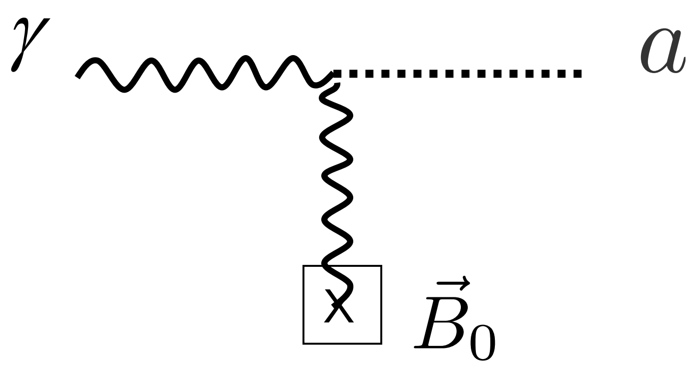

but rates for axion production and detection are proportional to $\left(\frac{1}{f_a}\right)^4$ and discouragingly small.

We may search for axions produced in the Sun or present on Earth as dark matter

- Axion helioscope

$$10^{14}\ \mathrm{axions/cm^2sec}$$

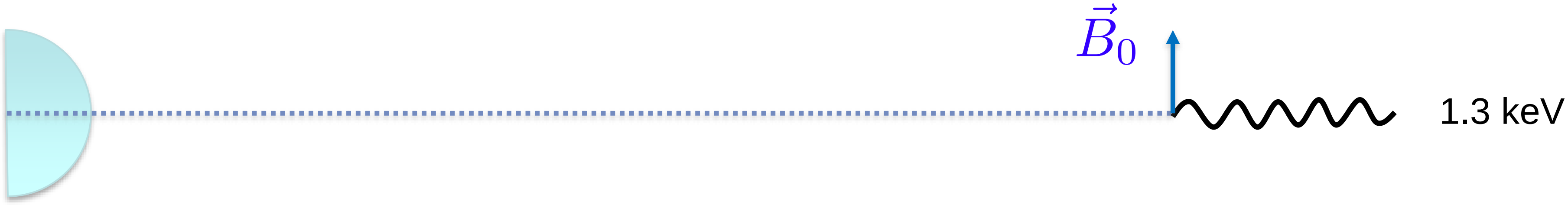

- Axion haloscope

$$10^{14}\ \mathrm{axions/cm^3}$$

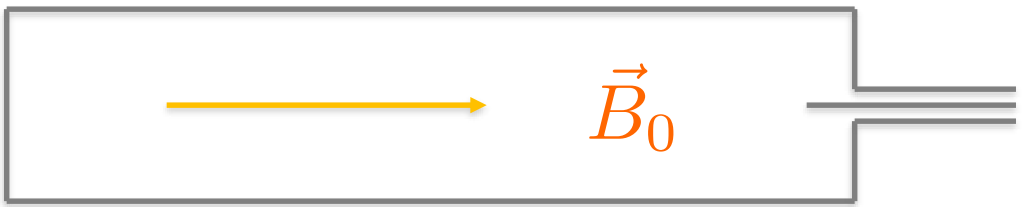

Axion dark matter is detectable

PS, 83

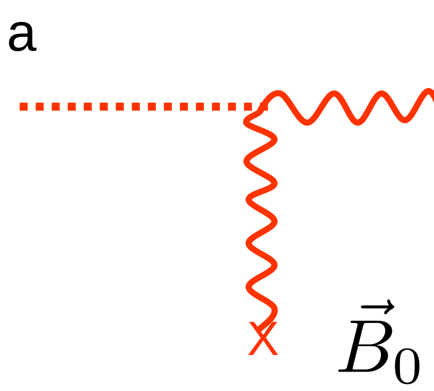

$$\mathcal{L}_{a\gamma\gamma} = -g_\gamma \frac{\alpha}{\pi}\frac{1}{f_a} a(x)\vec{E}(x)\cdot\vec{B}(x)$$

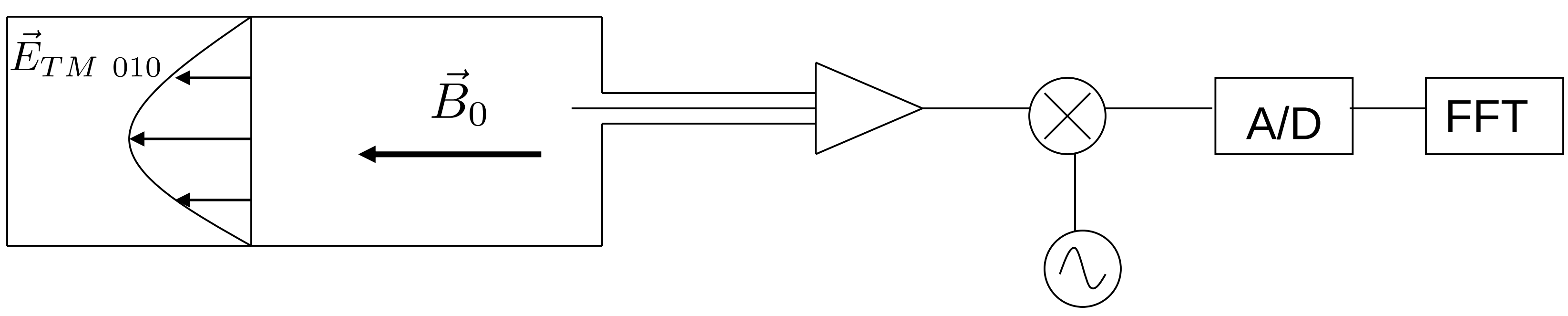

$$h\nu = m_a c^2 (1 + \frac{1}{2}\beta^2)$$

$$\beta = \frac{v}{c} \simeq 10^{-3}$$

$$Q_a \simeq 10^6$$

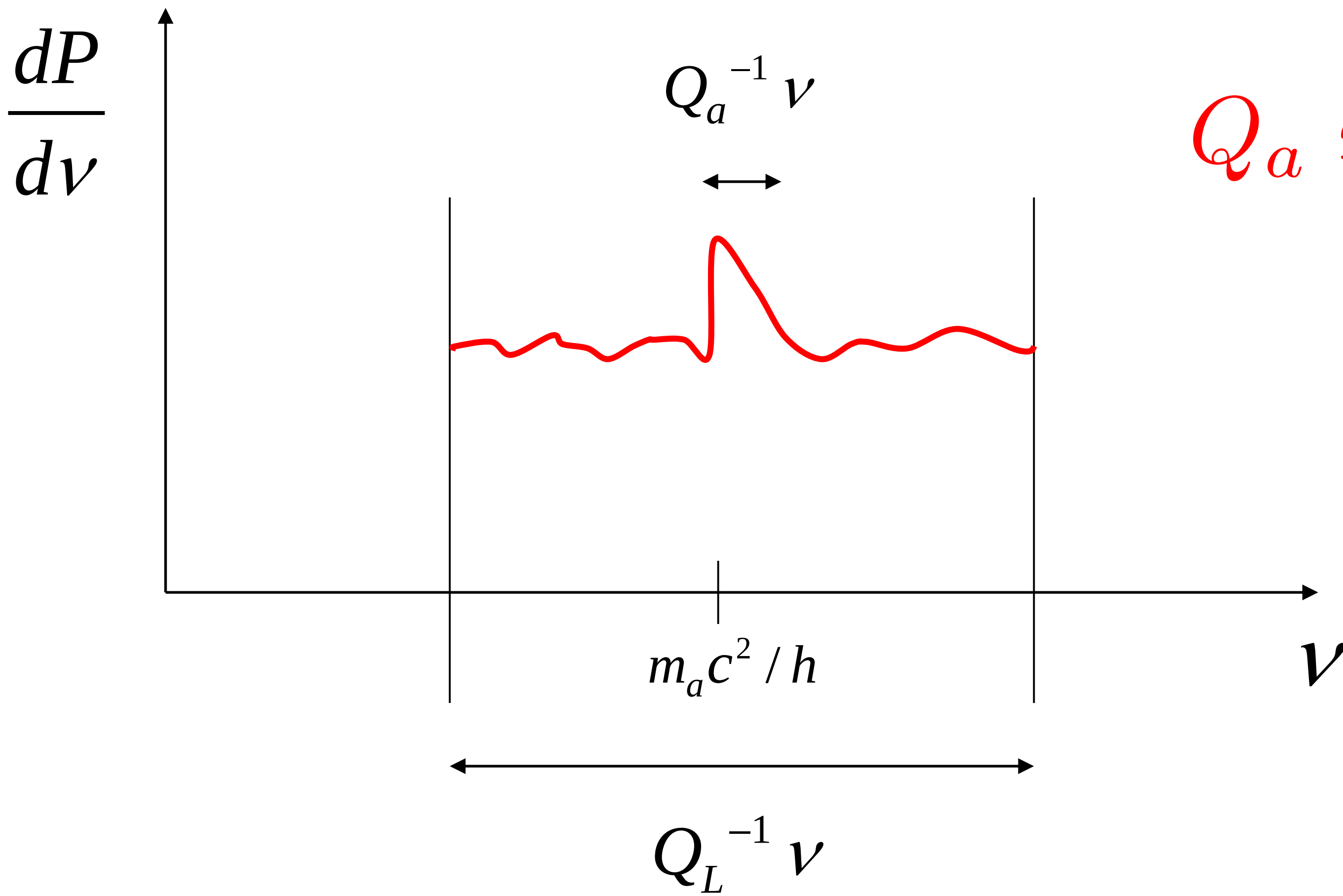

$$a \rightarrow \gamma$$

conversion power on resonance

$$P = \left(\frac{\alpha g_\gamma}{\pi f_a}\right)^2 V B_0{}^2 \rho_a C m_a{}^{-1} Q_L$$

$$= 2\cdot 10^{-22}\ \text{Watt} \left(\frac{V}{500\ \text{liter}}\right)\left(\frac{B_0}{7\ \text{Tesla}}\right)^2\left(\frac{C}{0.4}\right)$$

$$\left(\frac{g_\gamma}{0.36}\right)^2\left(\frac{\rho_a}{5\cdot 10^{-25}\ \text{gr/cm}^3}\right)\left(\frac{m_a c^2}{h\ \text{GHz}}\right)\left(\frac{Q_L}{10^5}\right)$$

search rate for s/n = 4

$$\frac{df}{dt} = \frac{1.2\ \text{GHz}}{\text{year}}\left(\frac{P}{2\cdot 10^{-22}\ \text{Watt}}\right)^2\left(\frac{3\,K}{T_n}\right)^2$$

Axion Dark Matter eXperiment

Magnet with Insert (side view)

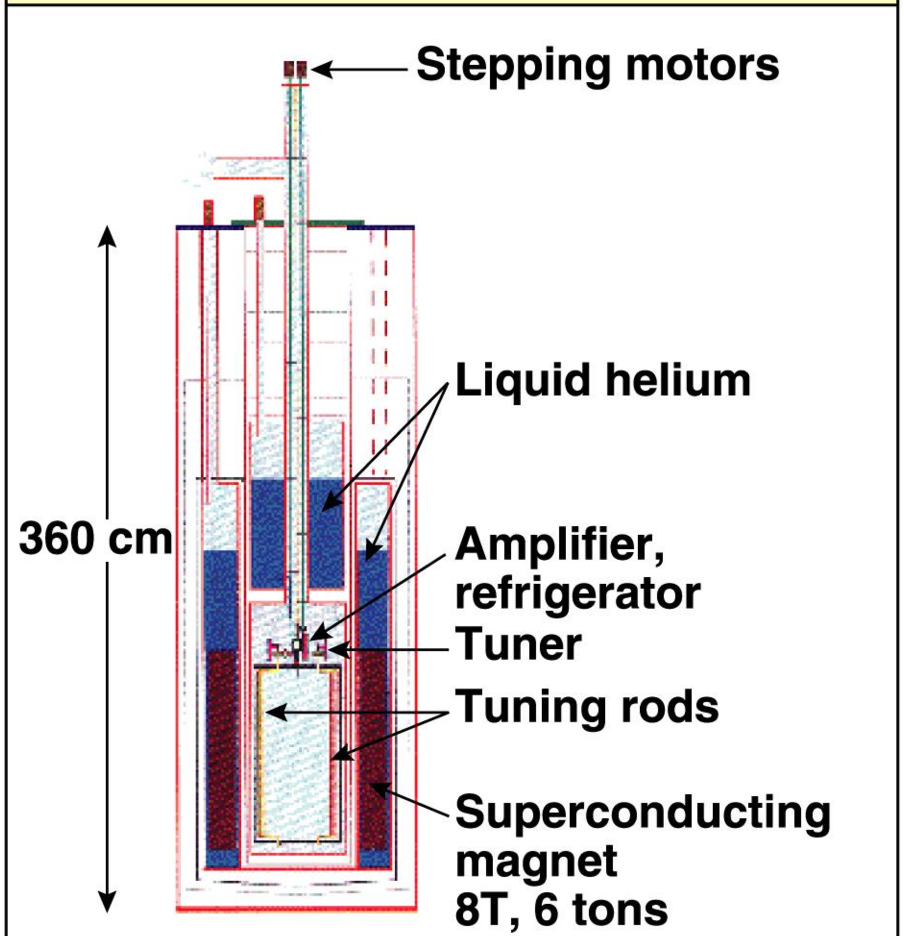

Pumped LHe → T ~ 1.5 k

Magnet

8 T, 1 m × 60 cm ∅

ADMX hardware

high Q cavity

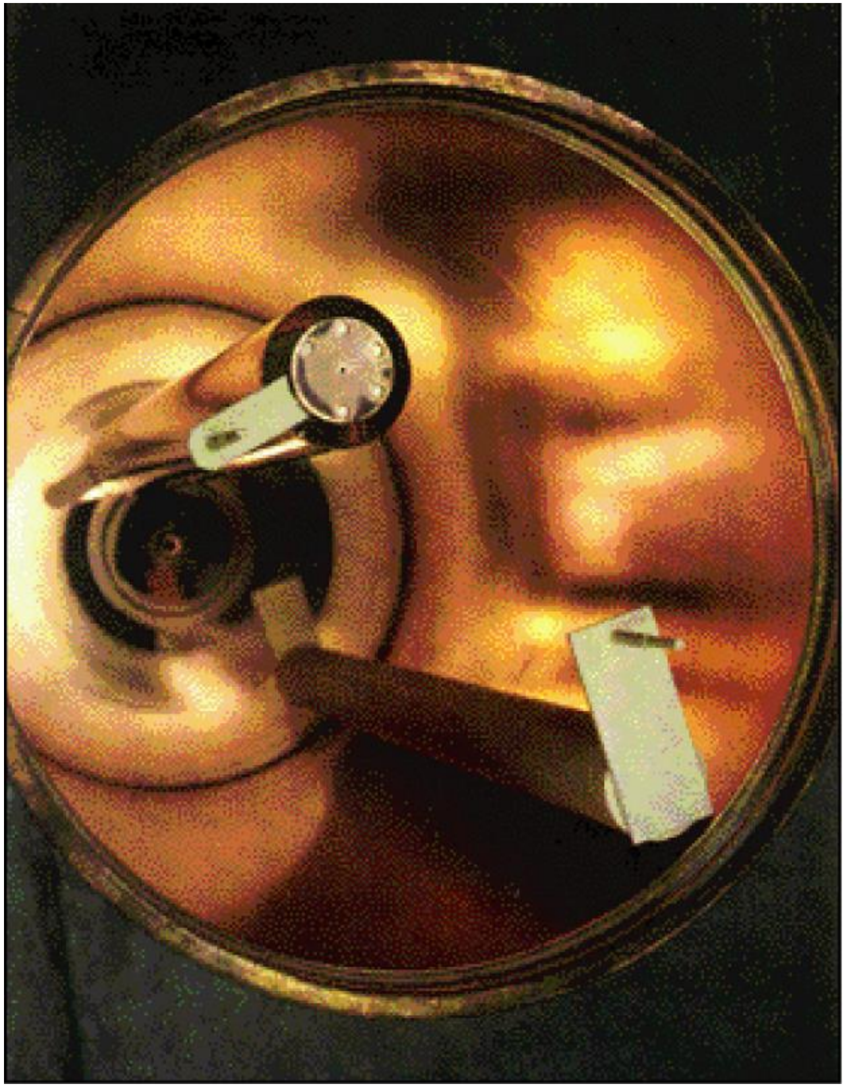

experimental insert

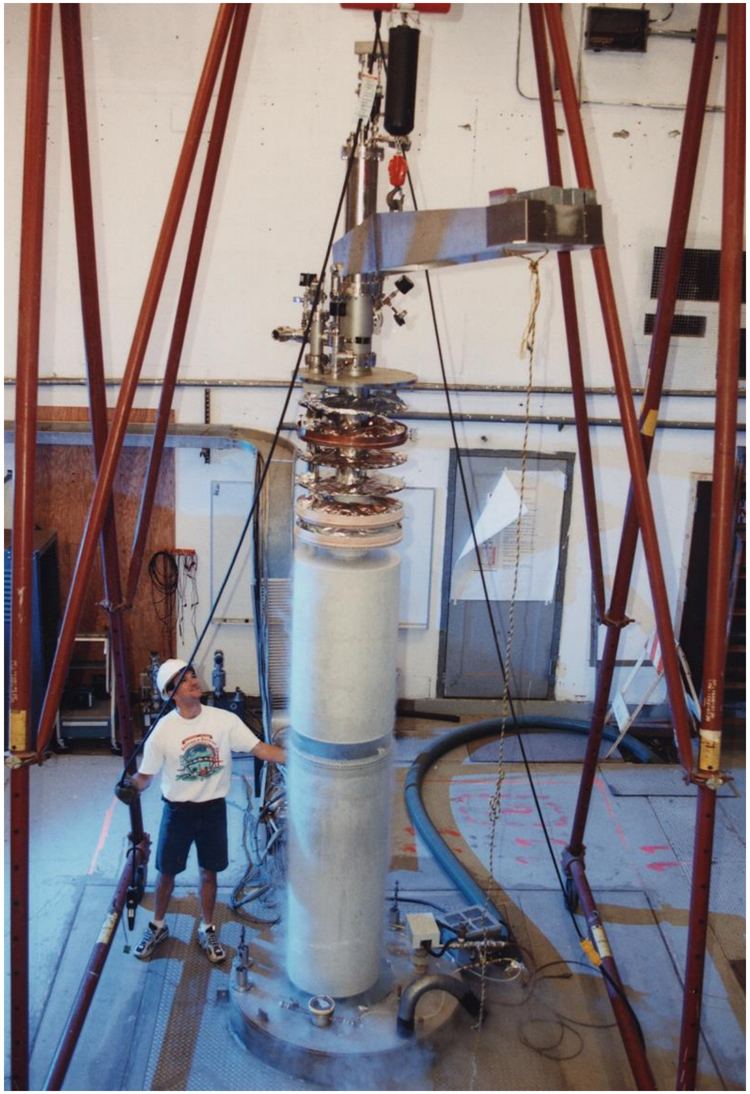

ADMX 2nd generation

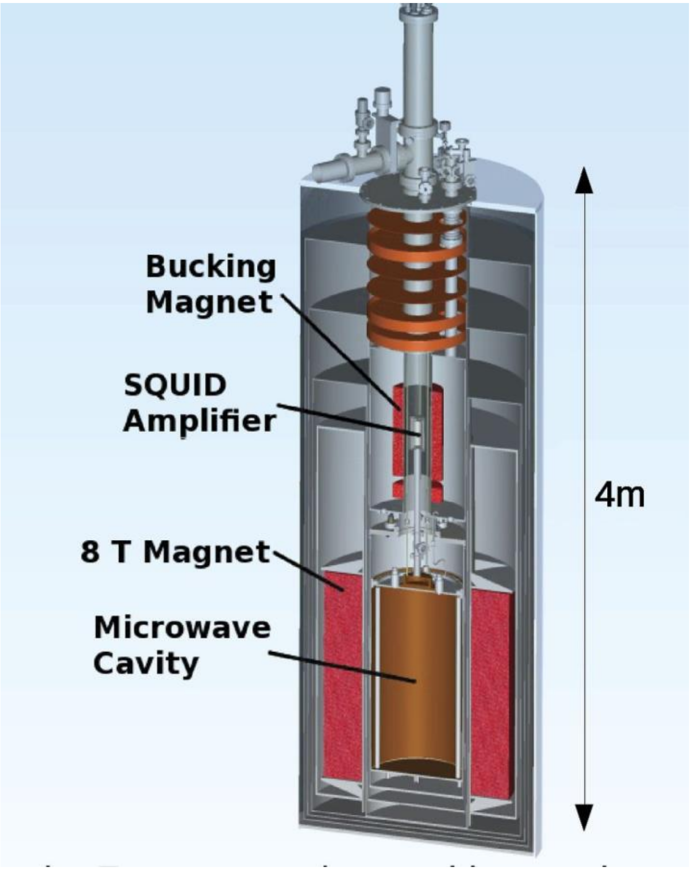

SQUIDs from
J. Clarke's group

Leslie Rosenberg and
Gray Rybka at U. Wash.

ADMX meeting at Fermilab

HAYSTAC at Yale

Institute for Basic Science
ibs
기초과학연구원

CAPP

Center for
Axion and Precision
Physics Research

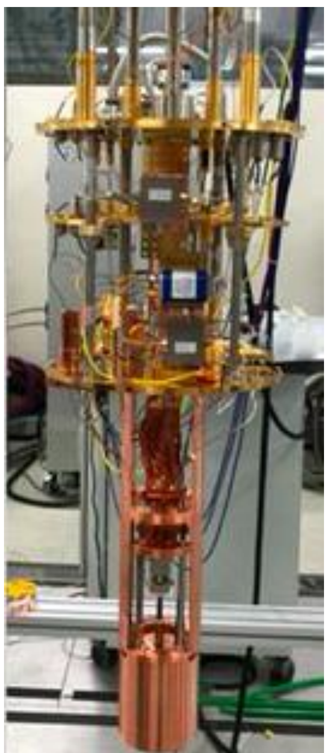

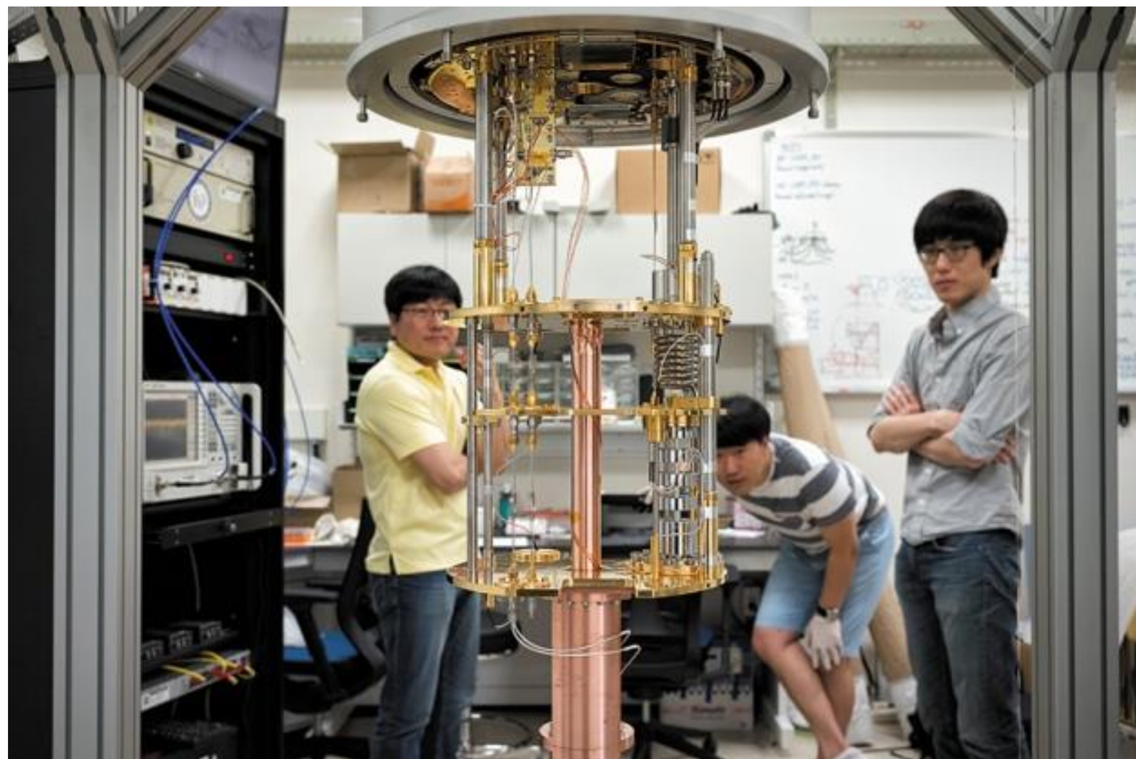

Cavity haloscopes

- ADMX in Seattle & FNAL
- HAYSTAC at Yale
- CAPP in Korea
- QUAX at INFN laboratory in Legnaro
- ORGAN at University of Western Australia
- RADES at CERN
- TASEH in Taiwan

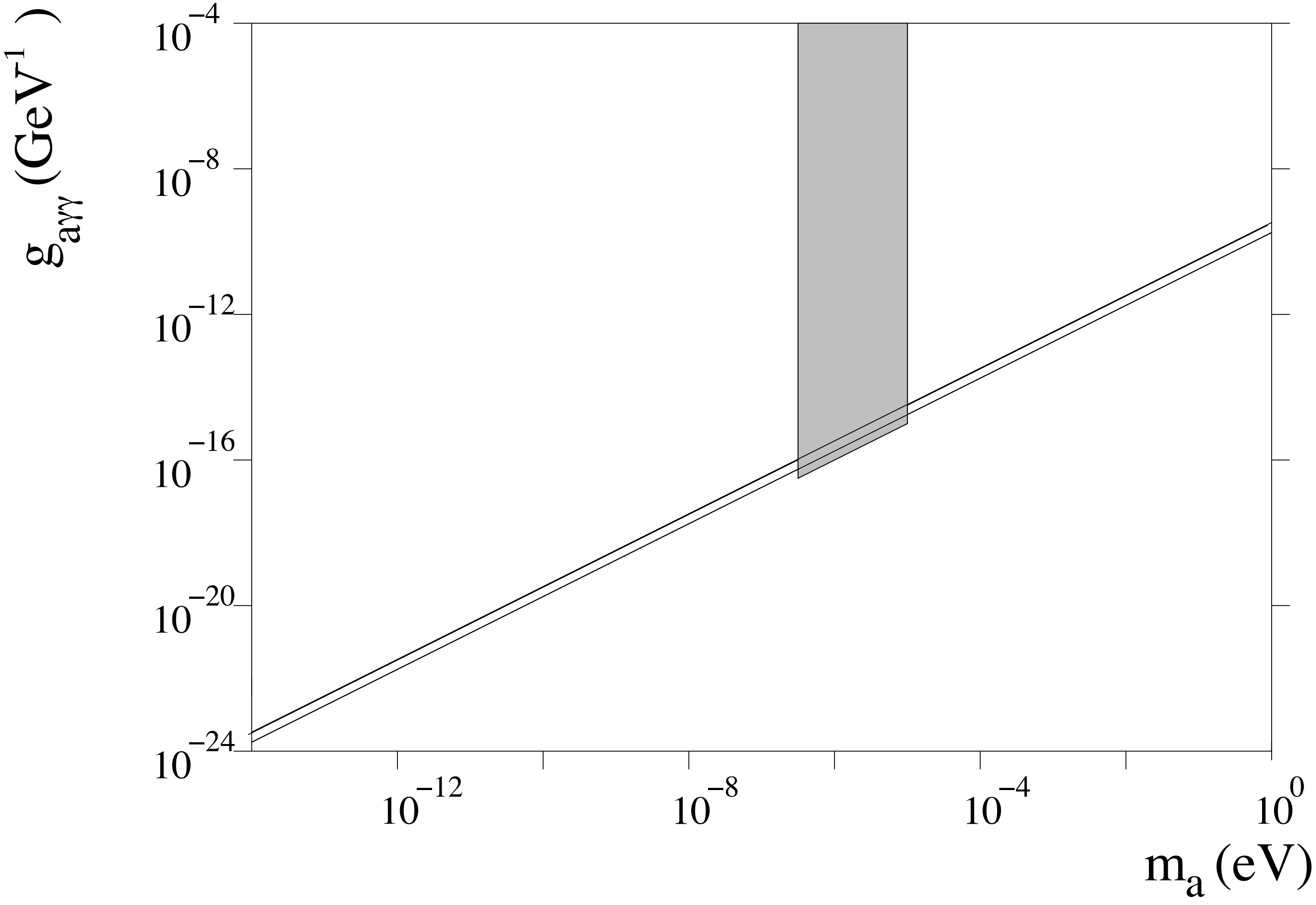

$$g_{a\gamma\gamma} = g_\gamma \frac{\alpha}{\pi} \frac{1}{f_a}$$

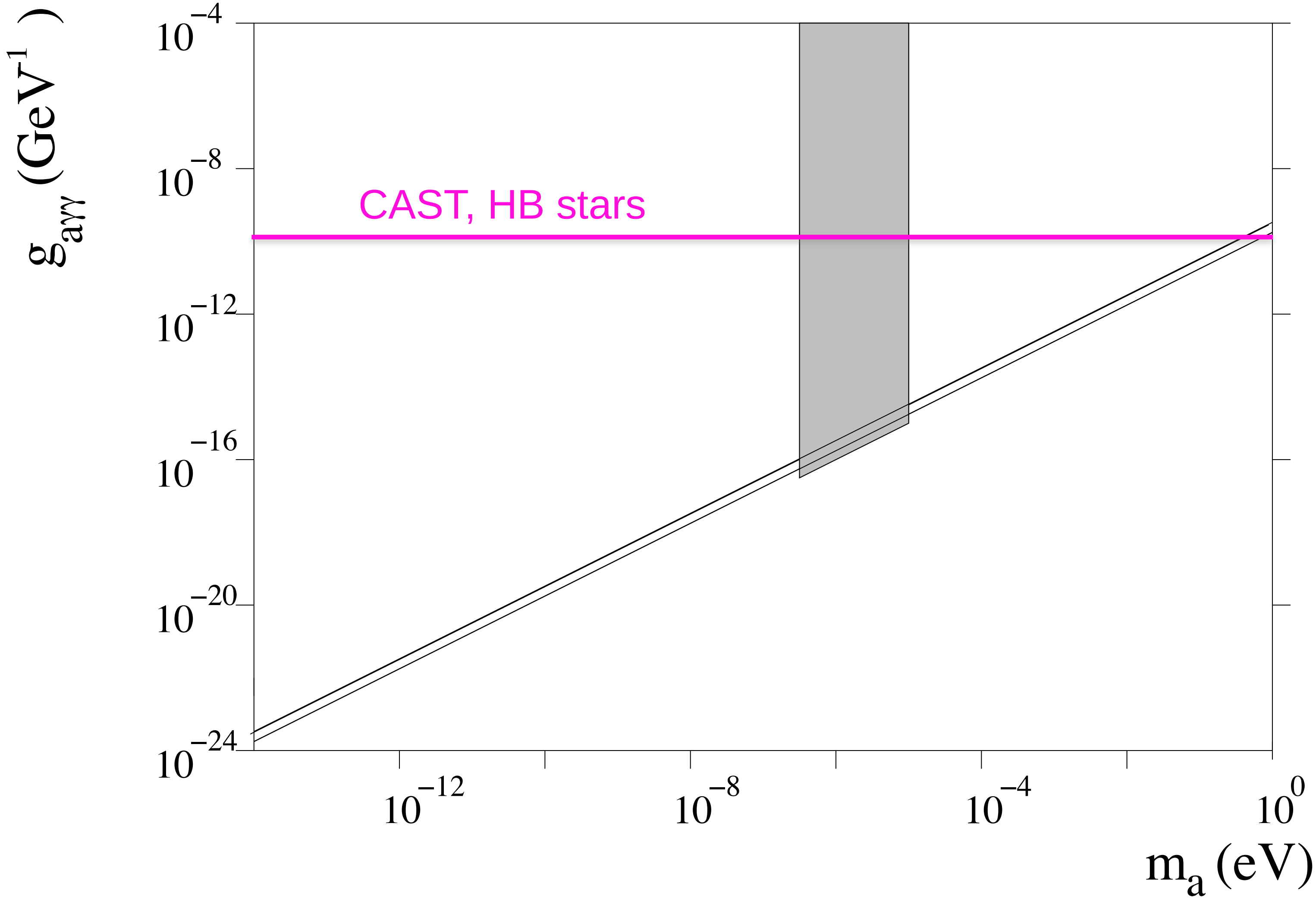

$$g_{a\gamma\gamma} = g_\gamma \frac{\alpha}{\pi} \frac{1}{f_a}$$

Constraints on dark matter axions from cavity haloscopes, in 2020

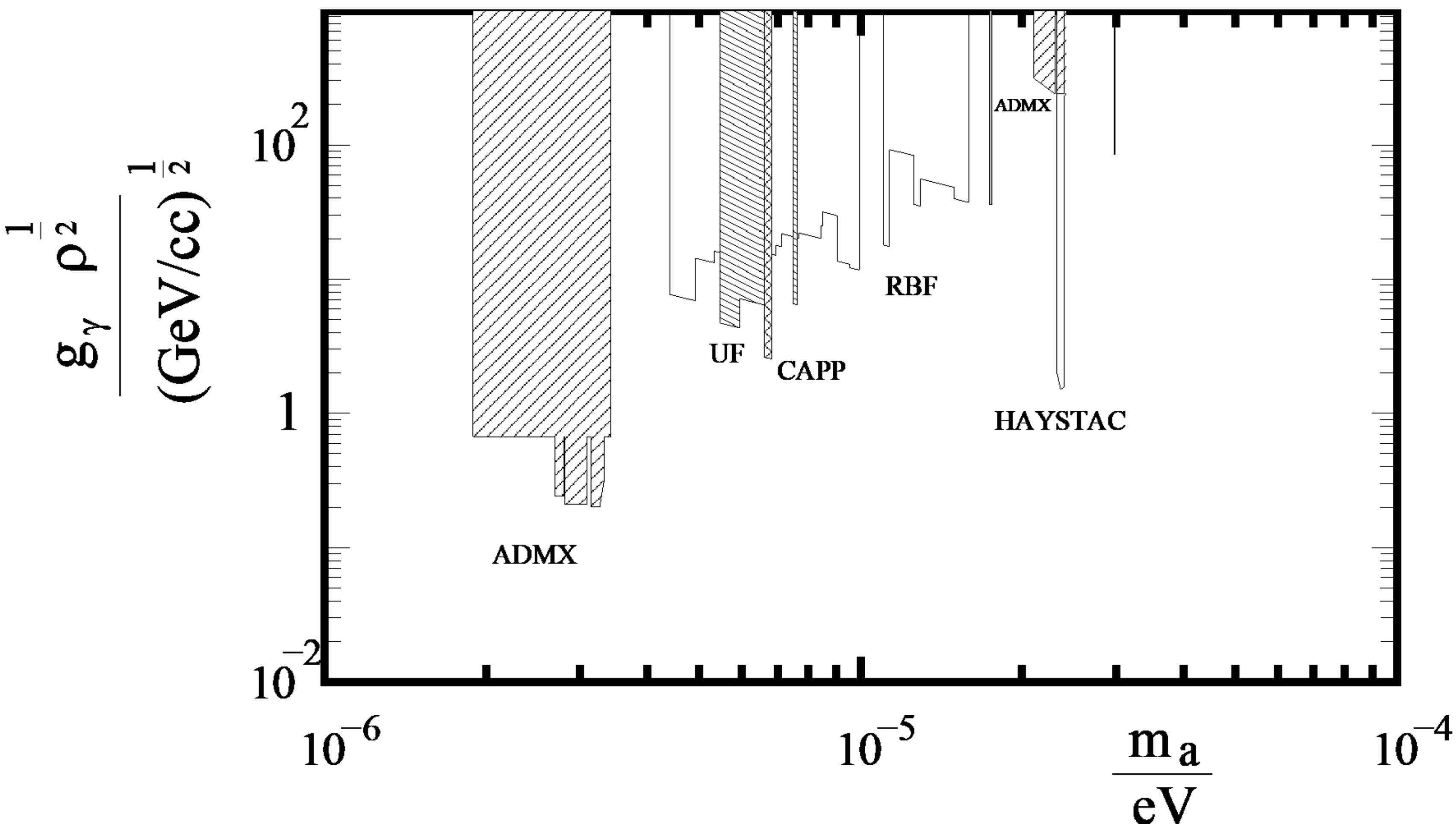

Axion photon constraints

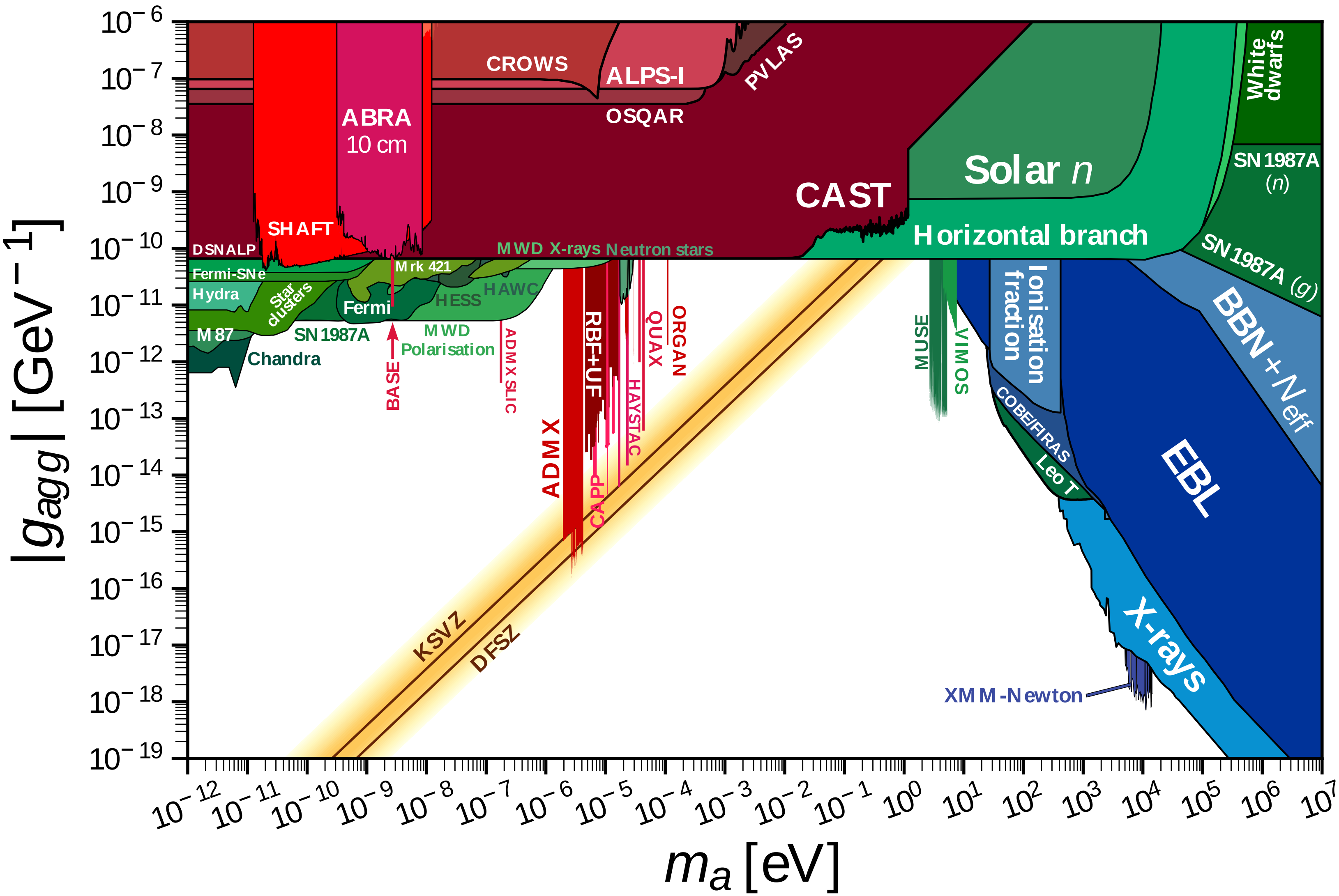

from https://cajohare.github.io/AxionLimits/ by Ciaran O'Hare

axion electrodynamics

the cavity haloscope

solar axion searches

shining light through walls

dielectric haloscopes

NMR methods

axion mediated long-range forces

LC circuit

axion echo

Axion to photon conversion in a magnetic field

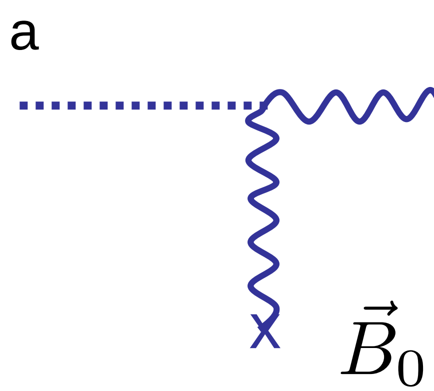

conversion probability

$$p(a \longleftrightarrow \gamma) = \left(\frac{\alpha\ g_\gamma}{\pi\ f_a}\right)^2 \mathrm{B}_0^{\ 2} \left(\frac{\sin \frac{q_z L}{2}}{q_z}\right)^2$$

with $$q_z = \frac{m_a^{\ 2} - \omega_{\mathrm{pl}}^{\ 2}}{2E_a}$$

Theory

- P. S. ’83
- L. Maiani, R. Petronzio and E. Zavattini ’86
- K. van Bibber et al. ’87
- G. Raffelt and L. Stodolsky, ‘88
- K. van Bibber et al. ’89

....

Experiment

- D. Lazarus et al. ’92
- R. Cameron et al. ‘93
- S. Moriyama et al. ’98, Y. Inoue et al. ’02
- K. Zioutas et al. 04
- E. Zavattini et al. 05

....

Tokyo Axion Helioscope

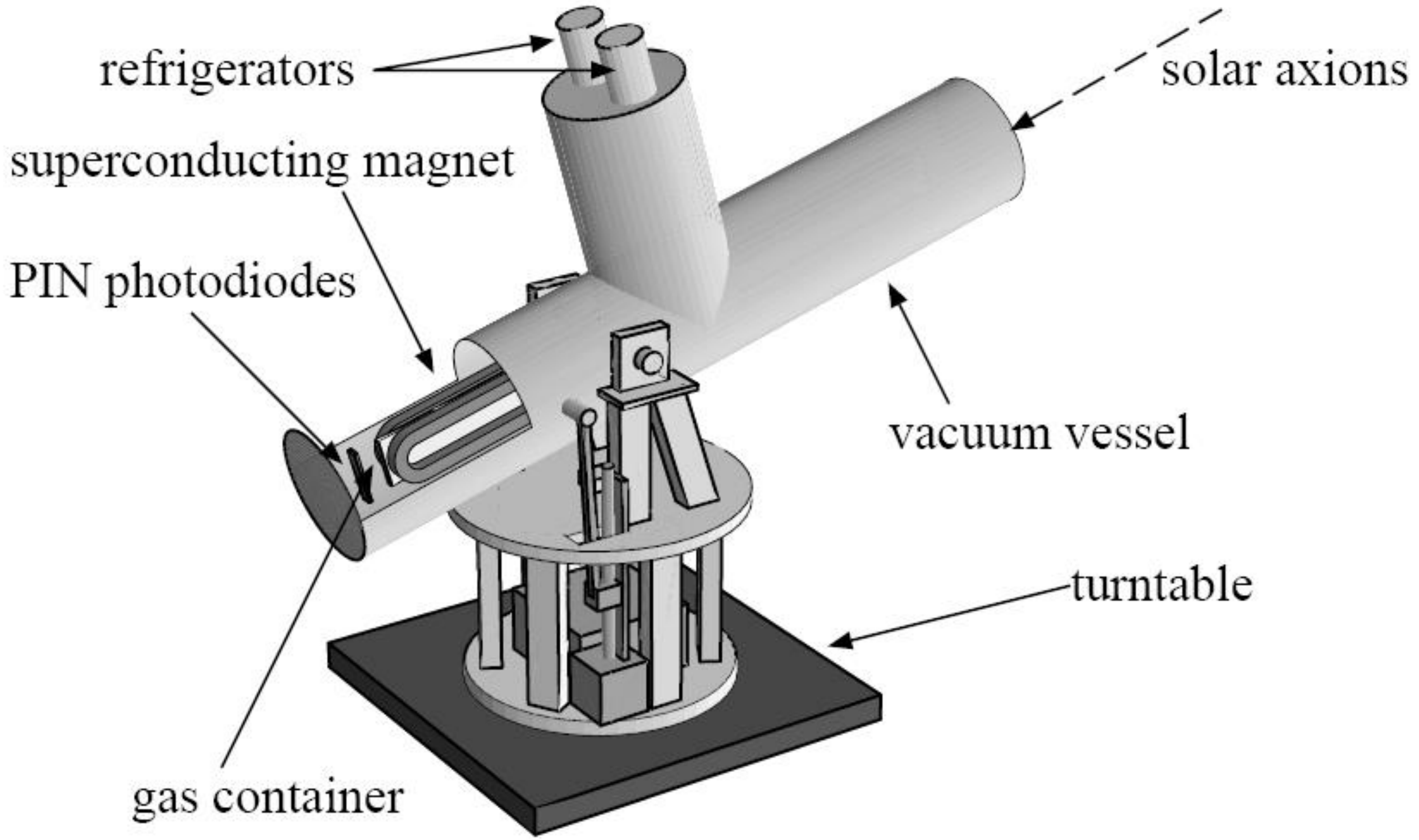

Cern Axion Solar Telescope

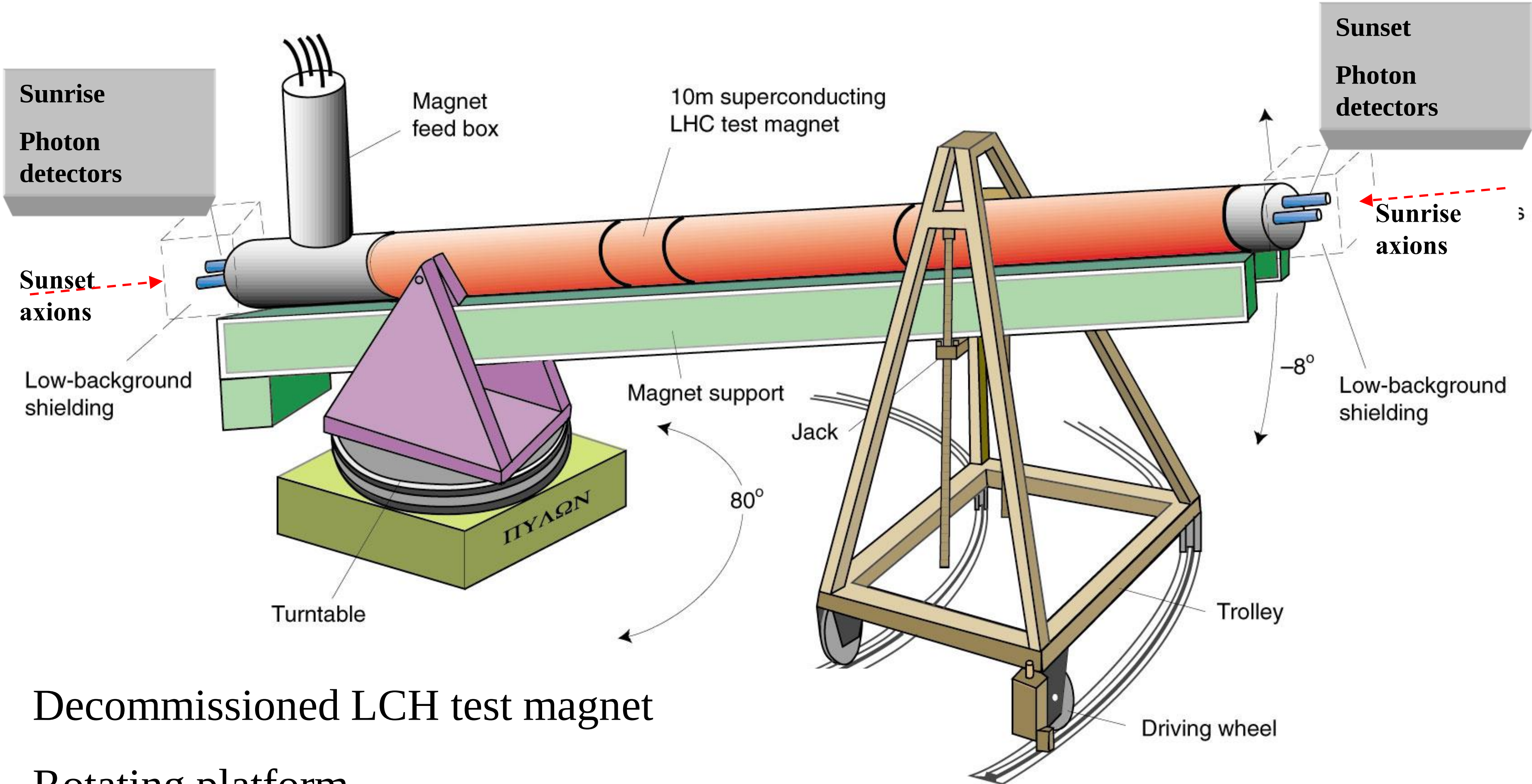

Decommissioned LCH test magnet

Rotating platform

3 X-ray detectors

X-ray Focusing Device


CAST
ANSALDO GIE
EUROPAMETALLI – LMI
E. ZANON

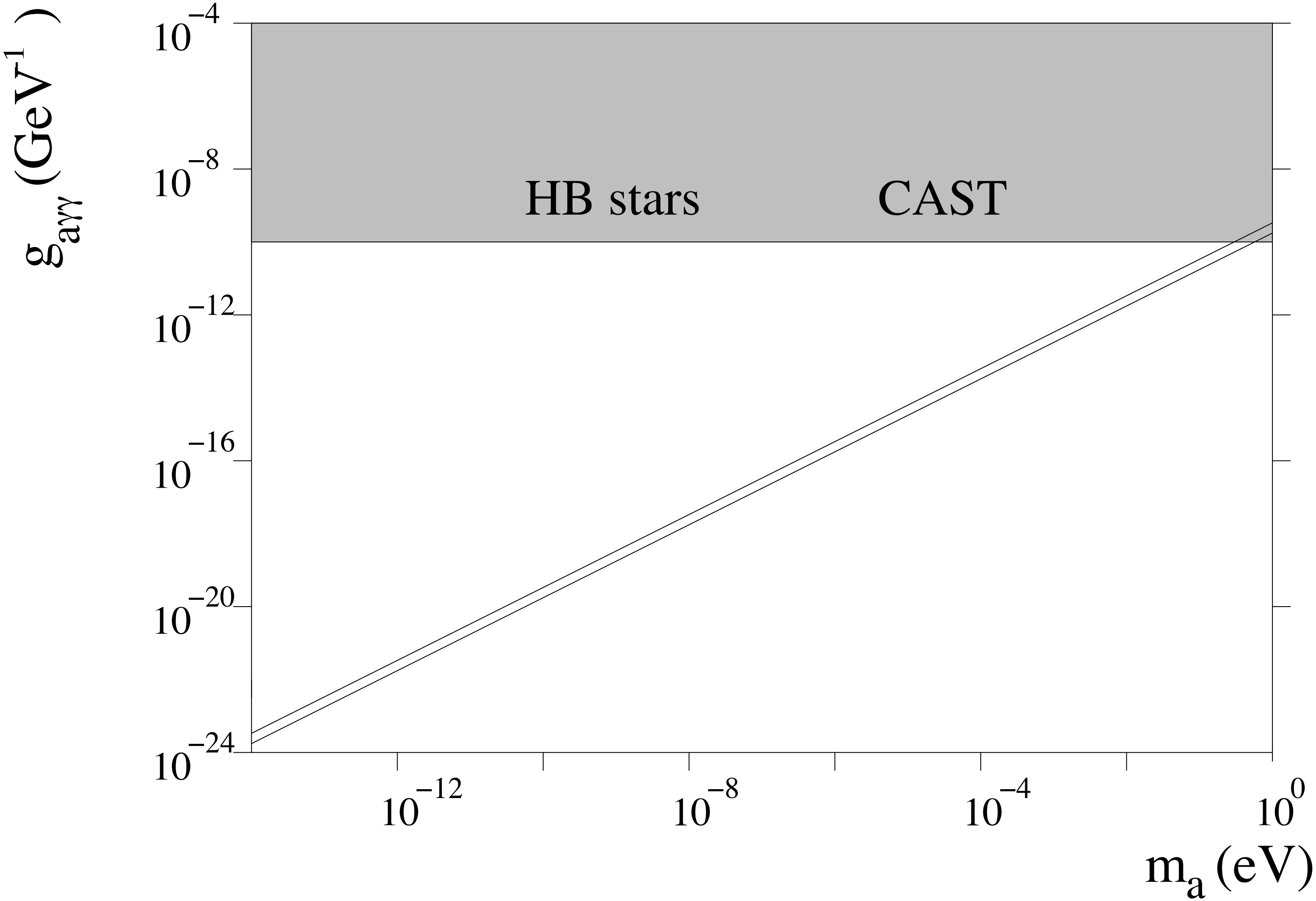

$g_{a\gamma\gamma}$ (GeV^{-1})
10^{-4}
10^{-8}
10^{-12}
10^{-16}
10^{-20}
10^{-24}
HB stars
CAST
10^{-12}
10^{-8}
10^{-4}
10^{0}
m_a (eV)

IAXO – Conceptual Design

- Large toroidal 8-coil magnet L = ~20 m
- 8 bores: 600 mm diameter each
- 8 x-ray optics + 8 detection systems
- Rotating platform with services

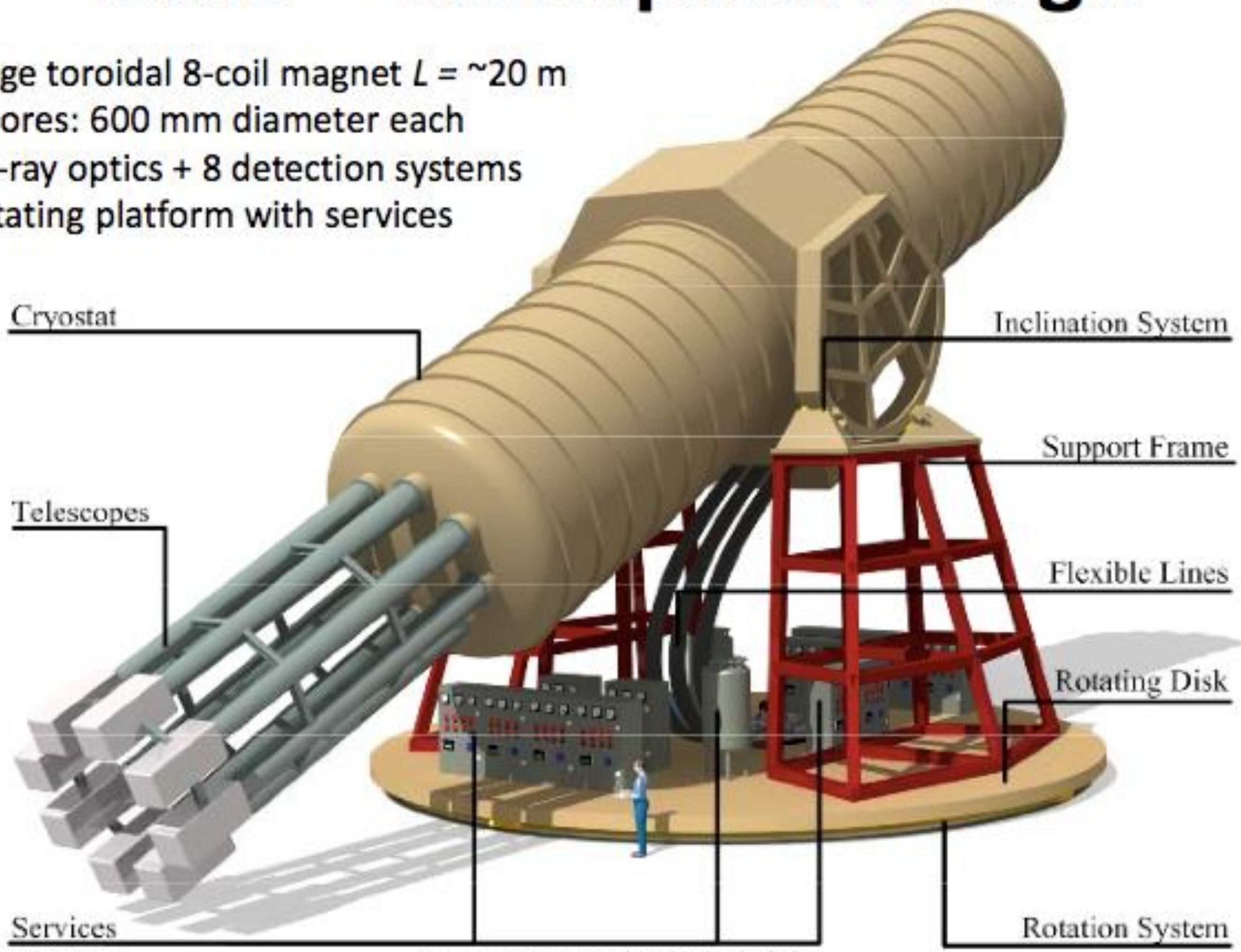

Baby IAXO at DESY

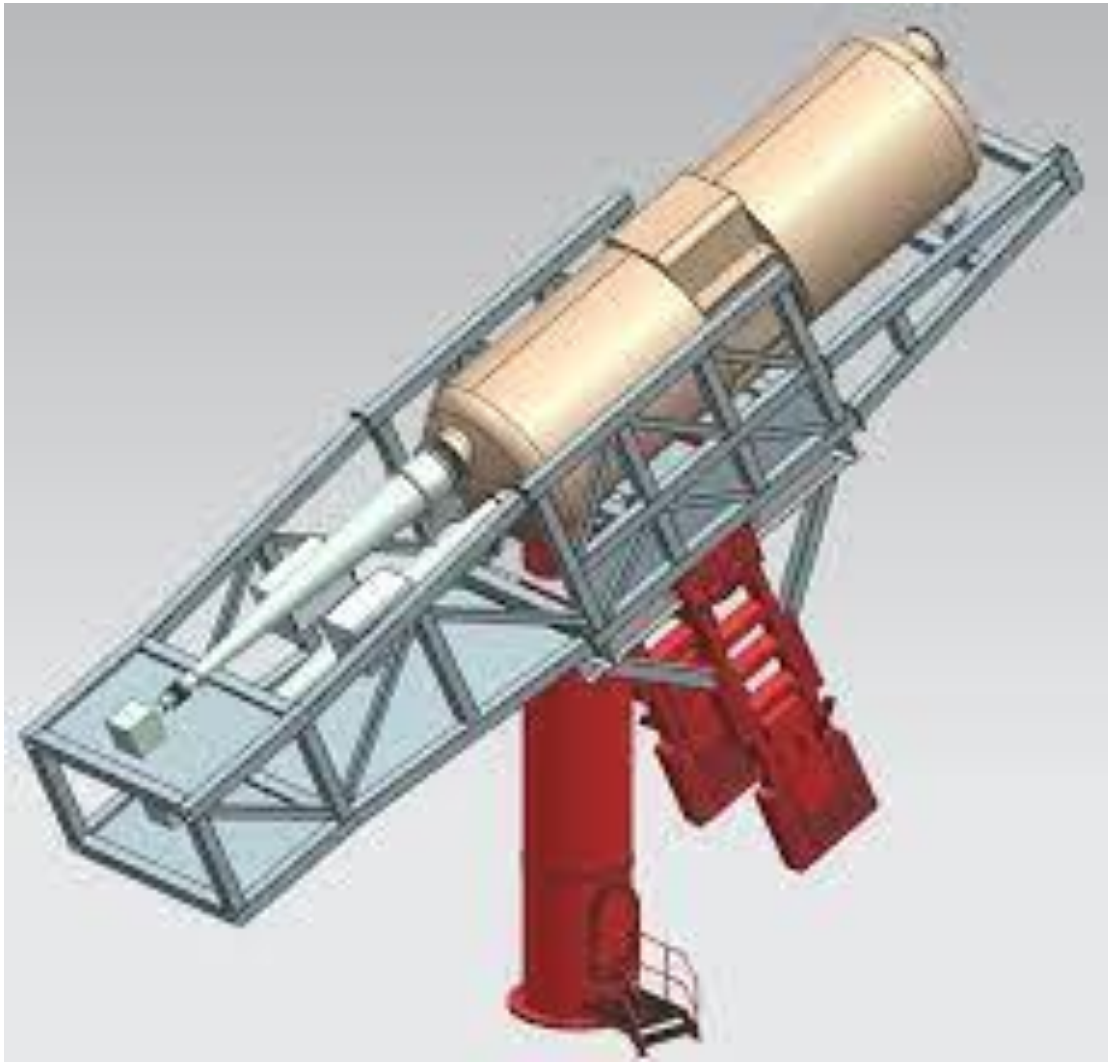

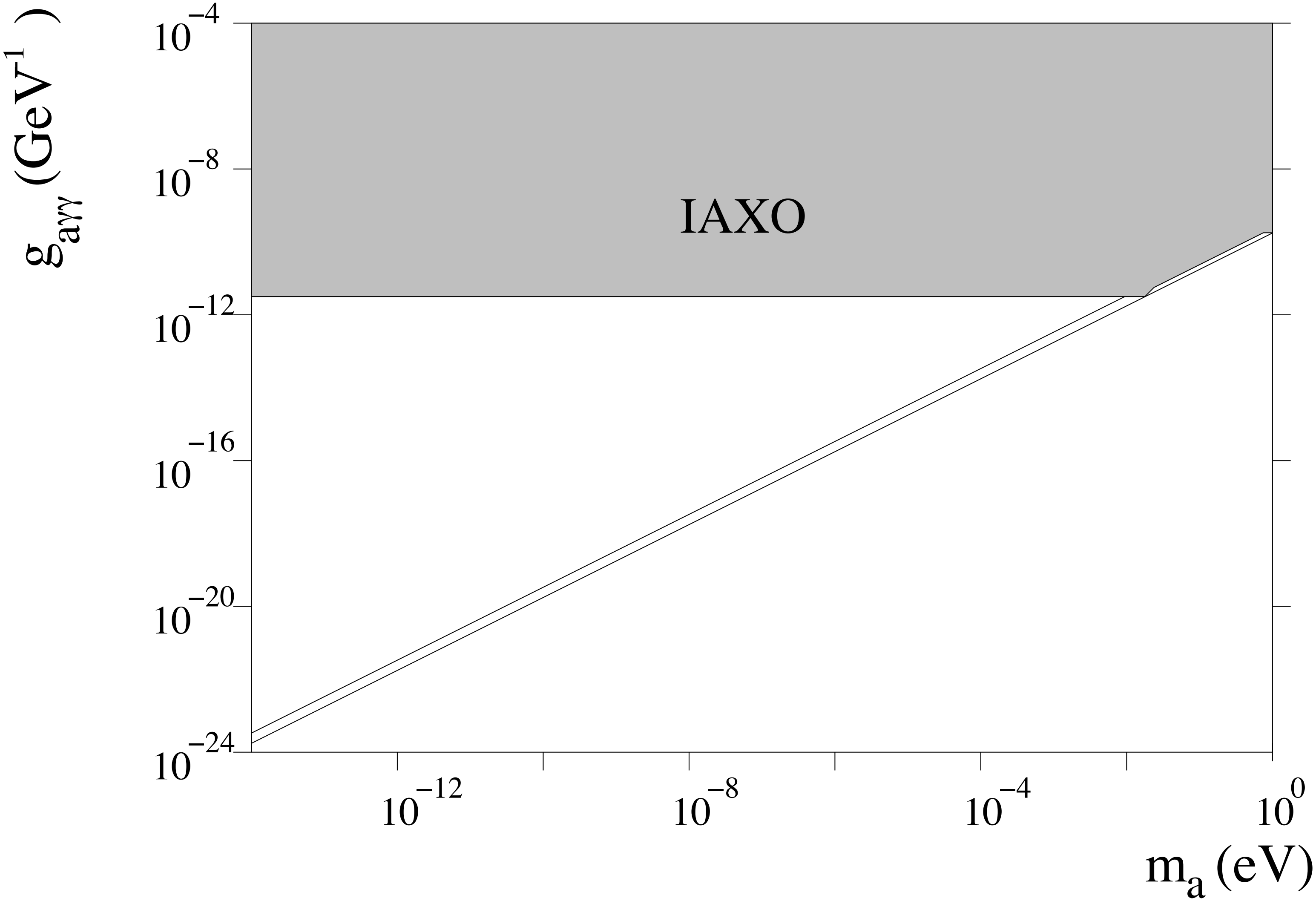

$g_{a\gamma\gamma}$ (GeV^{-1})
10^{-4}
10^{-8}
10^{-12}
10^{-16}
10^{-20}
10^{-24}
IAXO
10^{-12}
10^{-8}
10^{-4}
10^{0}
m_a (eV)

Axio-Electric and Primakoff Effects

$$a + \mathrm{Ge} \to e + \mathrm{Ge}^{+}$$

Dimopoulos, Starkman & Lynn, 1986

$$a + (Z, A) \to \gamma + (Z, A)$$

constraints from SOLAX, COSME, DAMA, CDMS, EDELWEISS, XMASS, CUORE, CDEX, Xenon, LUX, PandaX

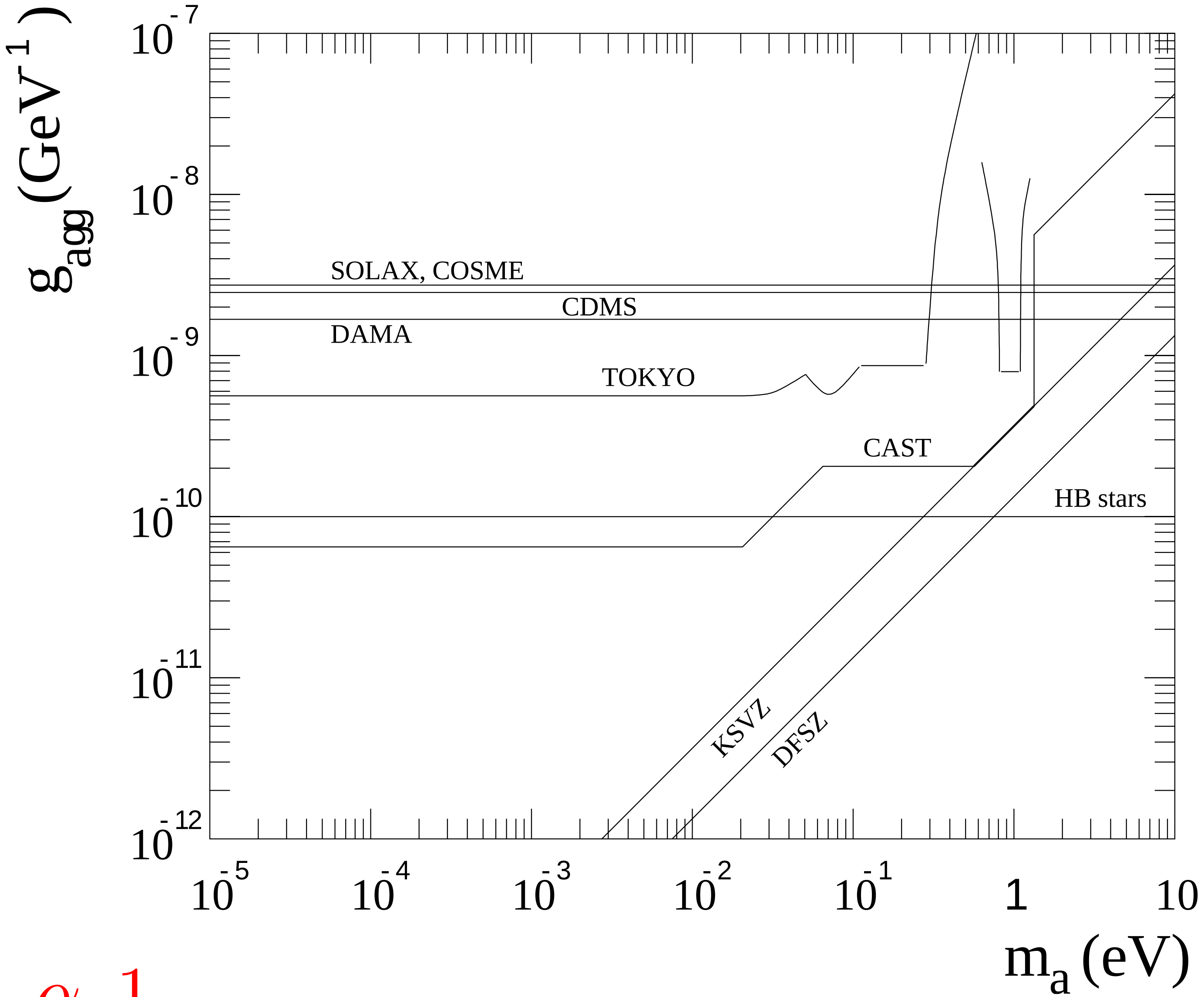

$$g_{a\gamma\gamma} = g_\gamma \frac{\alpha}{\pi} \frac{1}{f_a}$$

axion electrodynamics

the cavity haloscope

solar axion searches

shining light through walls

dielectric haloscopes

NMR methods

axion mediated long-range forces

LC circuit

axion echo

Shining light through walls

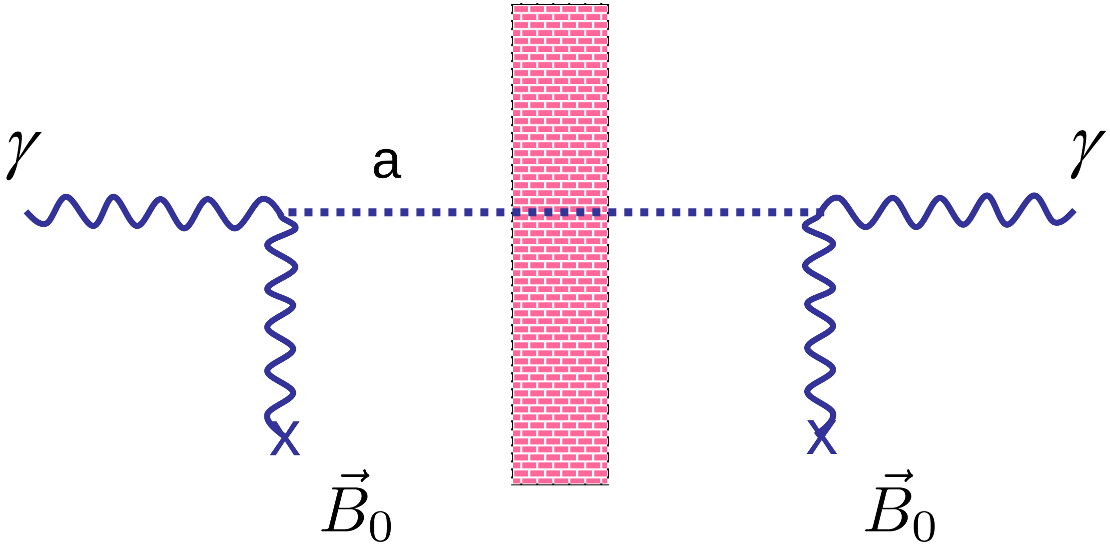

$$\text{rate} \propto \frac{1}{f_a^{\;4}}$$

K. van Bibber et al. ‘87

A. Ringwald ‘03

R. Rabadan,
A. Ringwald and
C. Sigurdson ‘05

P. Pugnat et al. '05

C. Robilliard et al. '07

A. Afanasev et al. '08

A. Chou et al. '08

K. Ehret et al. '10

Limits from "light through wall" axion searches

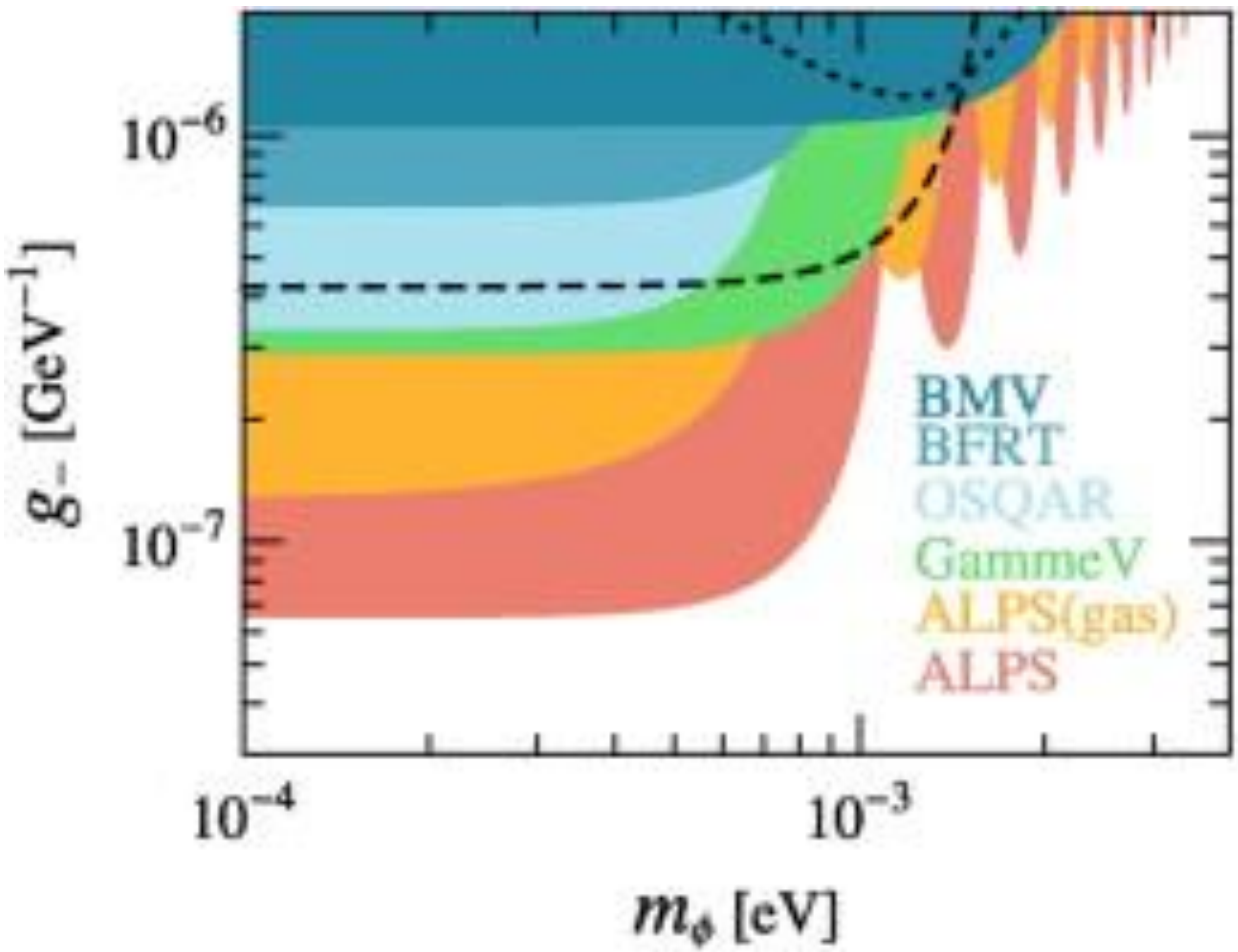

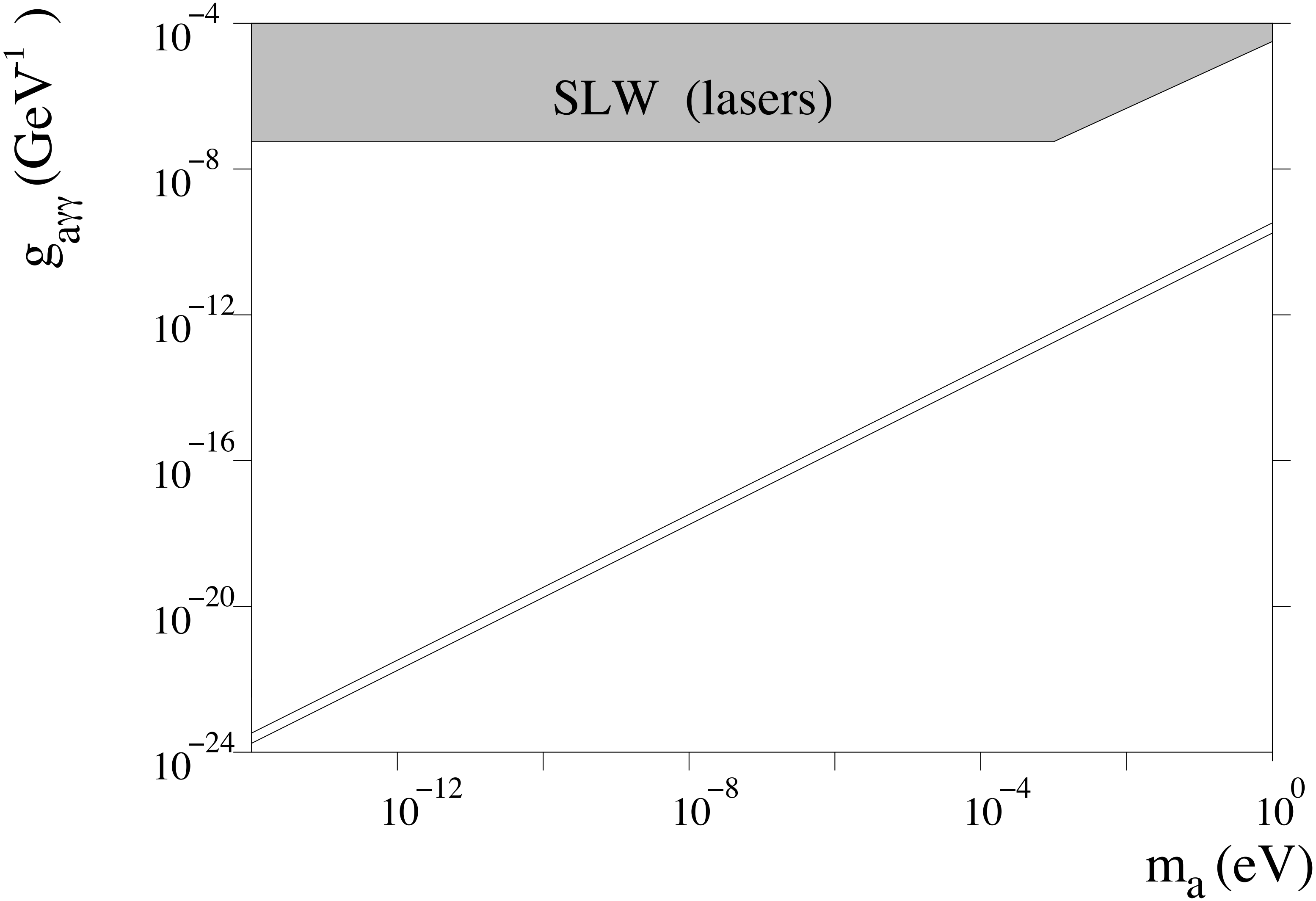

$g_{a\gamma\gamma}$ (GeV^{-1})
10^{-4}
10^{-8}
10^{-12}
10^{-16}
10^{-20}
10^{-24}
SLW (lasers)
10^{-12}
10^{-8}
10^{-4}
10^{0}
m_a (eV)

Resonantly Enhanced Axion-Photon Regeneration

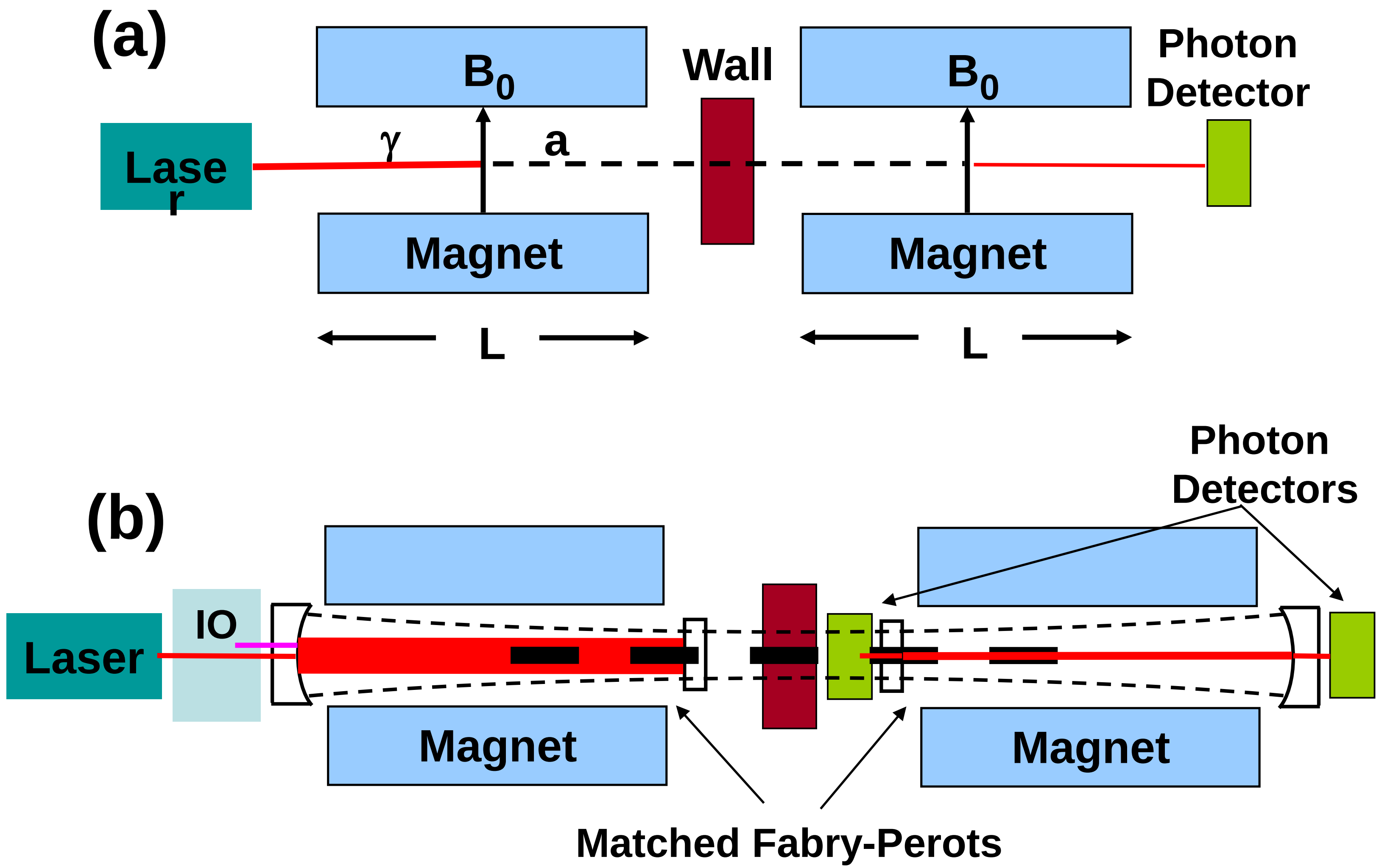

Hoogeveen (1996); P.S., Tanner and van Bibber (2007) & G. Mueller (2009)

ALPS II at DESY

A. Ringwald, A. Lindner et al.

$B_0 = 5.3 \text{ T} \quad L = 2 \times 120 \ m$ in HERA tunnel

ALPS II at DESY

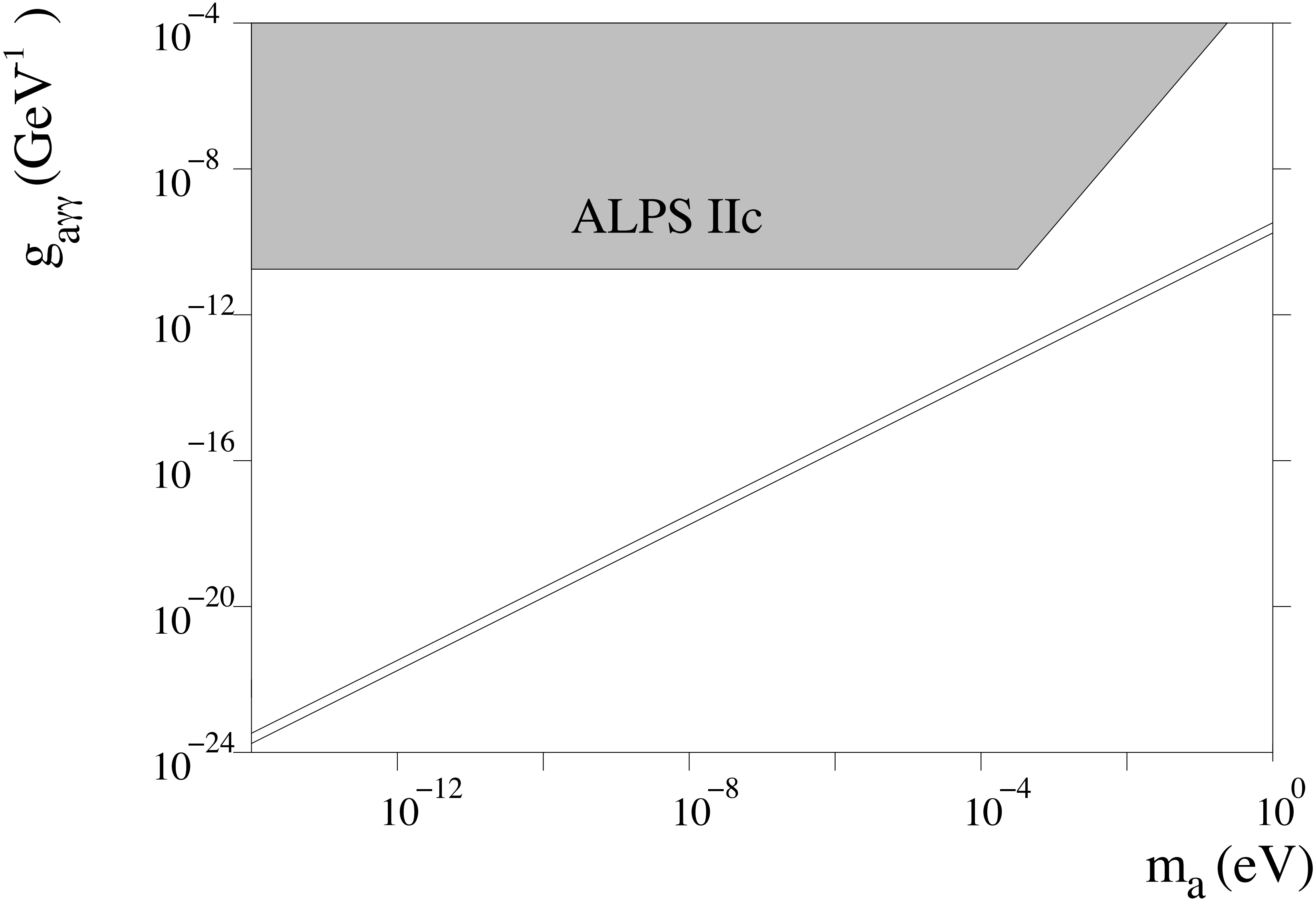

$g_{a\gamma\gamma}$ (GeV^{-1})
10^{-4}
10^{-8}
10^{-12}
10^{-16}
10^{-20}
10^{-24}
ALPS IIc
10^{-12}
10^{-8}
10^{-4}
10^{0}
m_a (eV)

Dish antenna

$$P \sim |\mathbf{E}|^2 A_{\rm dish} \sim 10^{-26} \left(\frac{\rm B}{\rm 5T} \frac{c_\gamma}{2} \right)^2 \frac{A_{\rm dish}}{1\,{\rm m}^2} {\rm Watt}$$

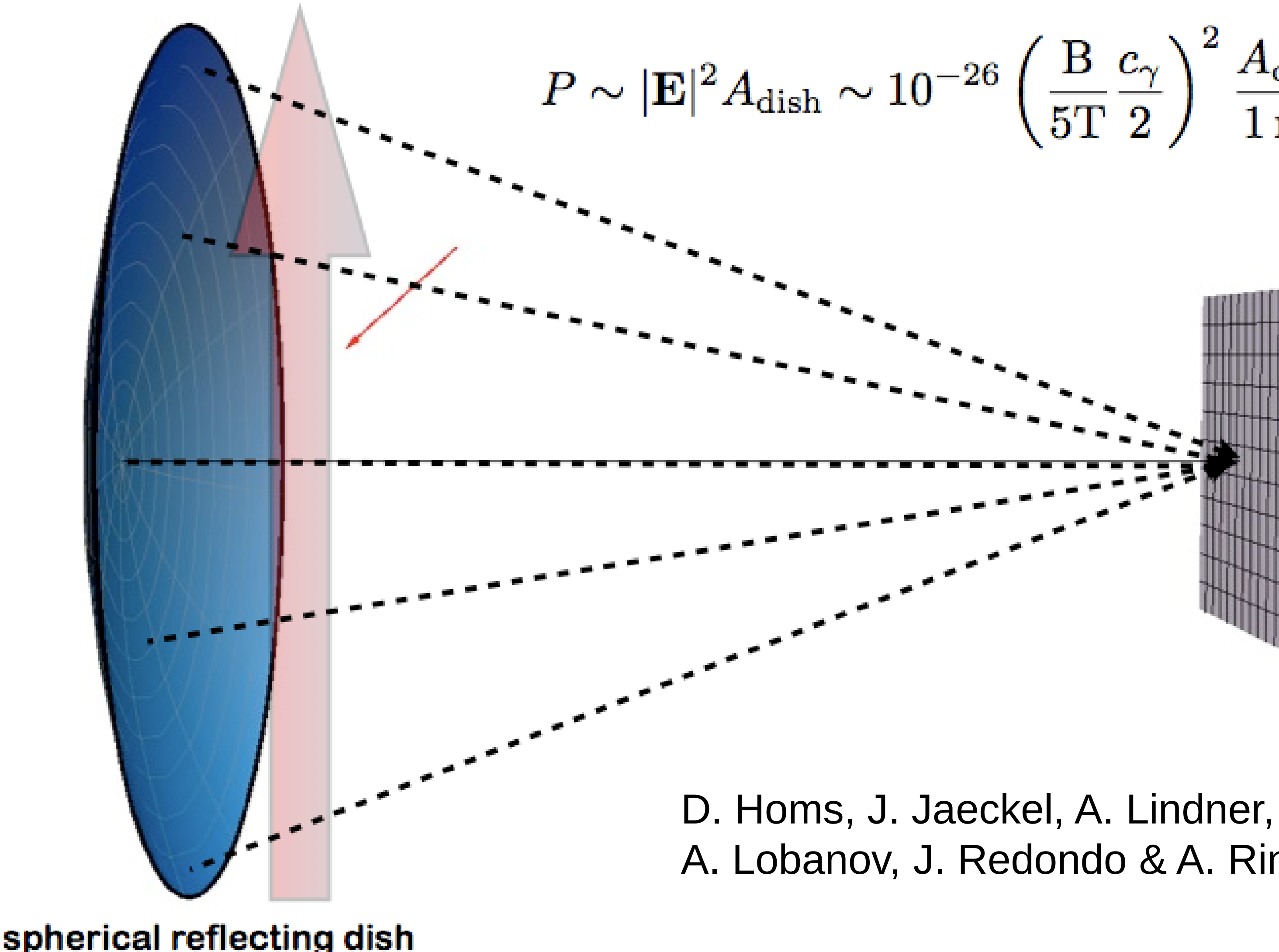

D. Homs, J. Jaeckel, A. Lindner,
A. Lobanov, J. Redondo & A. Ringwald, 2013

B. Doebrich et al. ,2014

Dielectric Haloscope

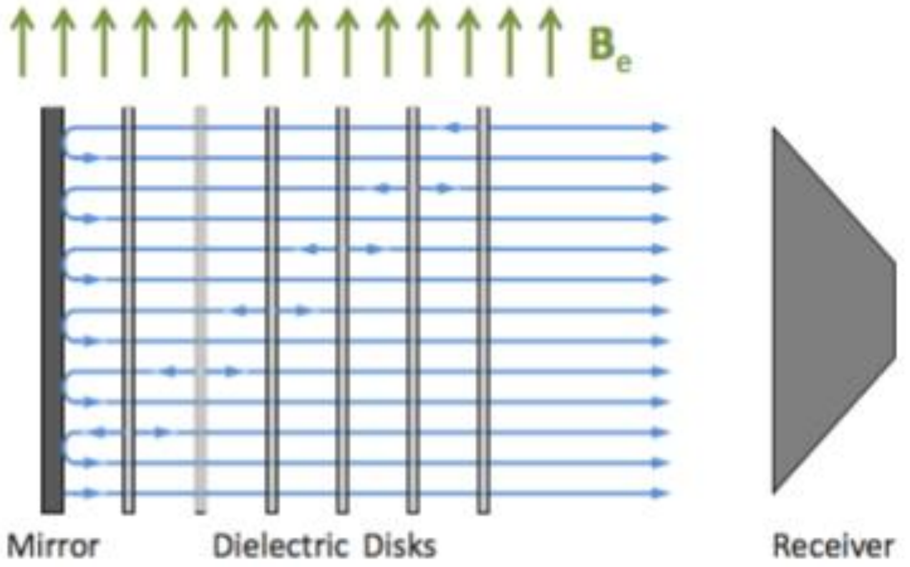

FIG. 1. A dielectric haloscope consisting of a mirror and several dielectric disks placed in an external magnetic field $\mathbf{B}_e$ and a receiver in the field-free region. A parabolic mirror (not shown) could be used to concentrate the emitted power into the receiver. Internal reflections are not shown.

MADMAX

MADMAX at DESY

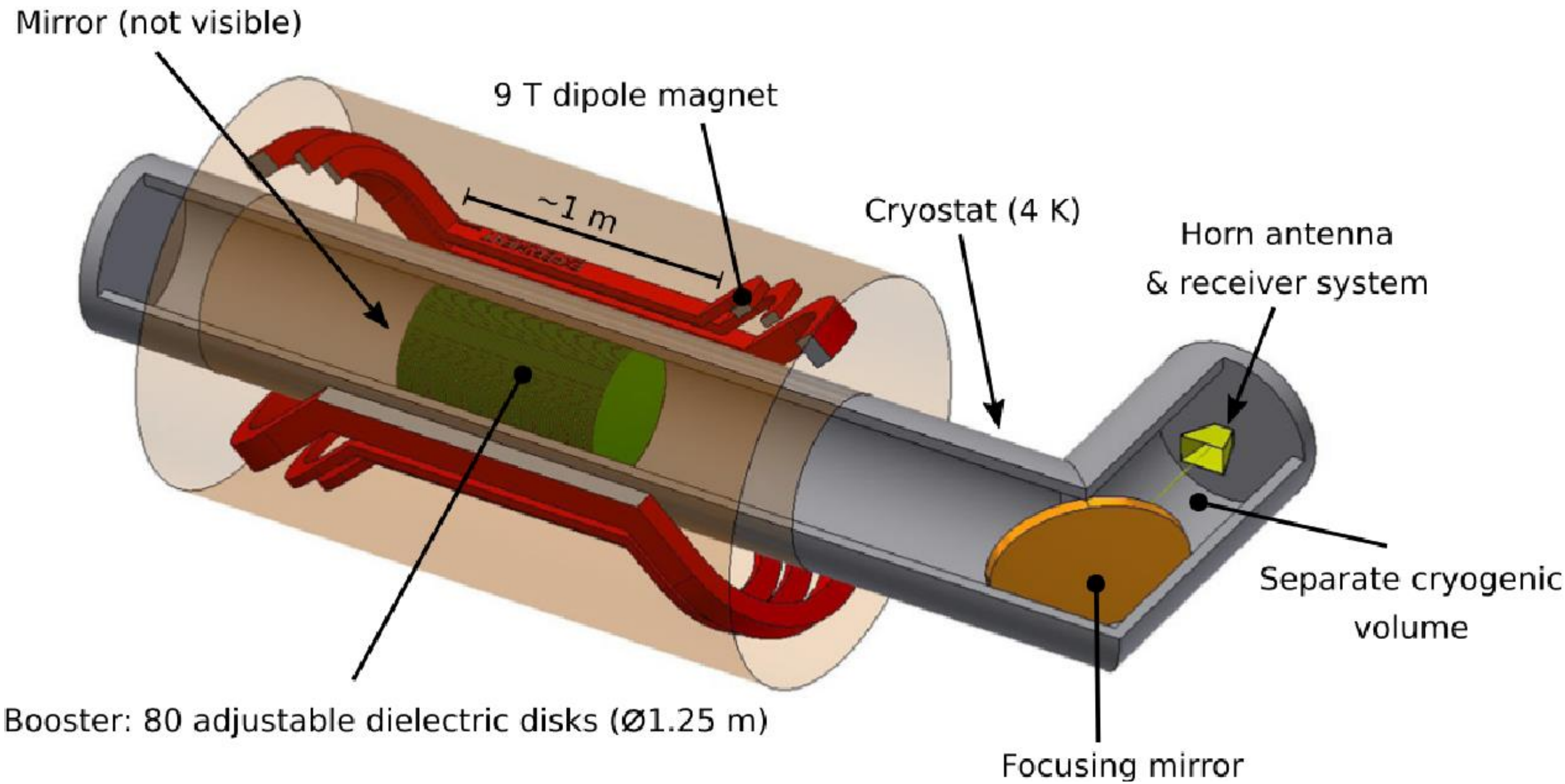

axion electrodynamics

the cavity haloscope

solar axion searches

shining light through walls

dielectric haloscopes

NMR methods

axion mediated long-range forces

LC circuit

axion echo

NMR techniques

P. Graham, S. Rajendran; D. Budker, M. Ledbetter, A. Sushkov

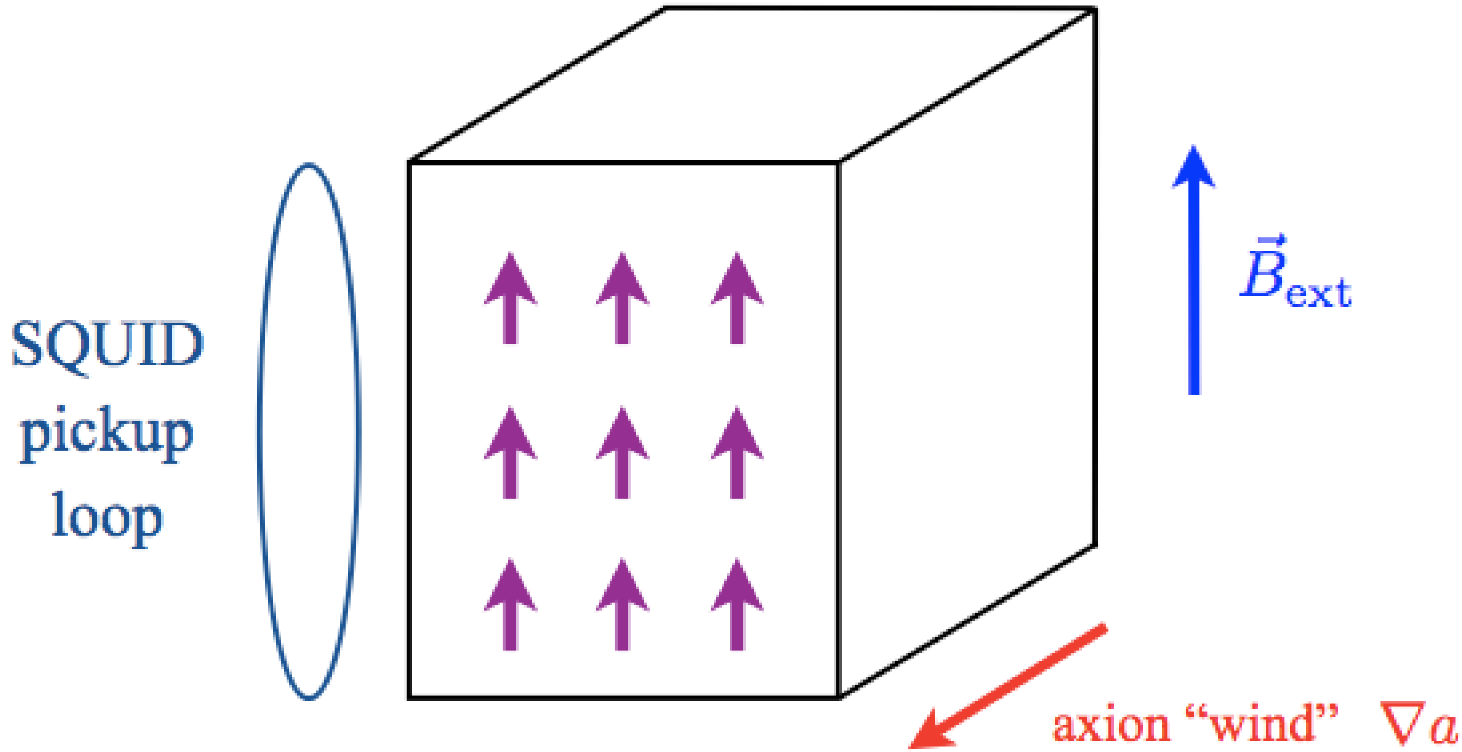

use nuclear spins coupled to axion DM

$$g_{\rm aNN}\,(\partial_\mu a)\,\bar{N}\gamma^\mu\gamma_5 N \implies H_N \supset g_{\rm aNN}\vec{\nabla}a.\vec{S}_N$$

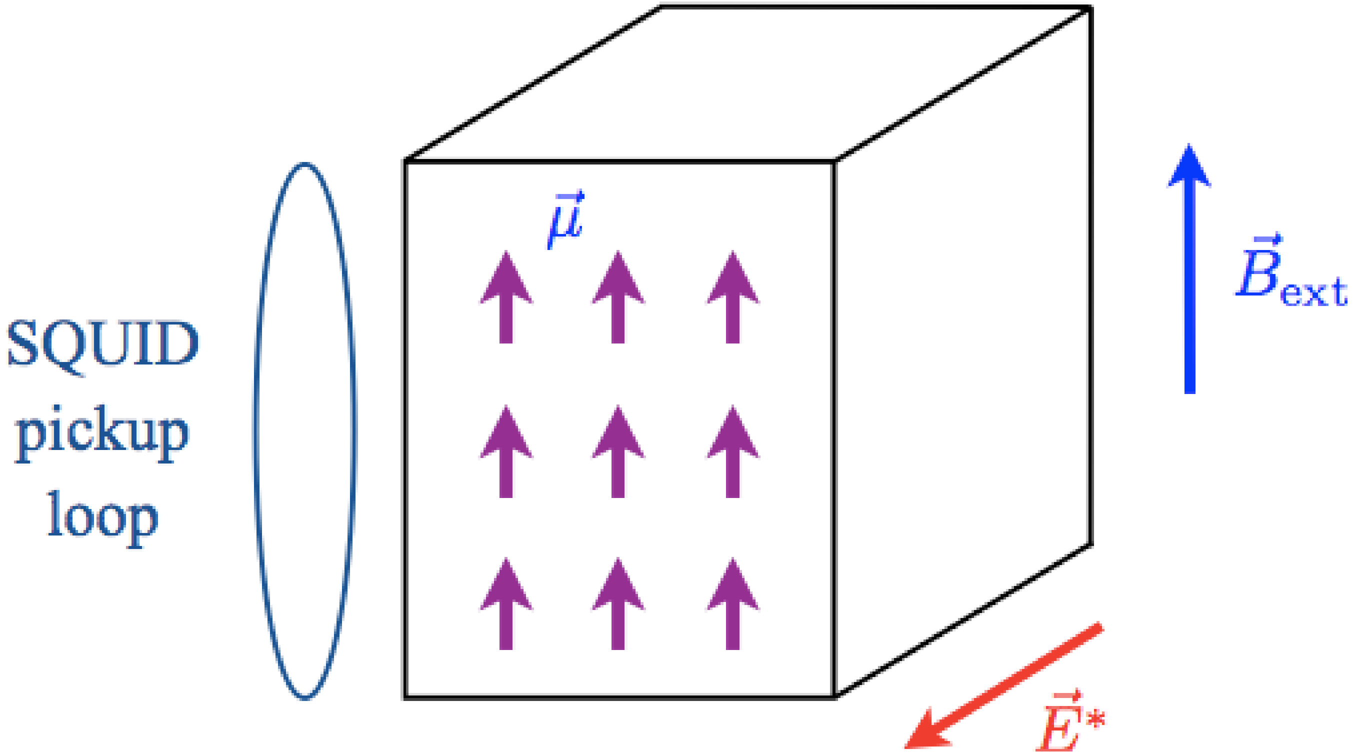

the axion field induces an oscillating nuclear electric dipole moment

$$d_e \sim 10^{-16}\ e\ \text{cm}\ \frac{a(x)}{f_a}$$

Macroscopic forces mediated by axions

$$L_{a\bar{f}f} = g_f \frac{m_f}{f_a} a \bar{f} \left(i\gamma_5 + \theta_f \right) f$$

forces coupled to
the f spin density

forces coupled to
the f number density

background of
magnetic forces

$$\theta_f \sim 10^{-17}$$

Theory:

J. Moody and
F. Wilczek '84

Experiment:

A. Youdin et al. '96
W.-T. Ni et al. '96

NMR with long range axion field

A. Arvanitaki and A. Geraci, 2014

$$H_{\text{int}} = \frac{g_f m_f \theta_f}{f_a} a(x)$$

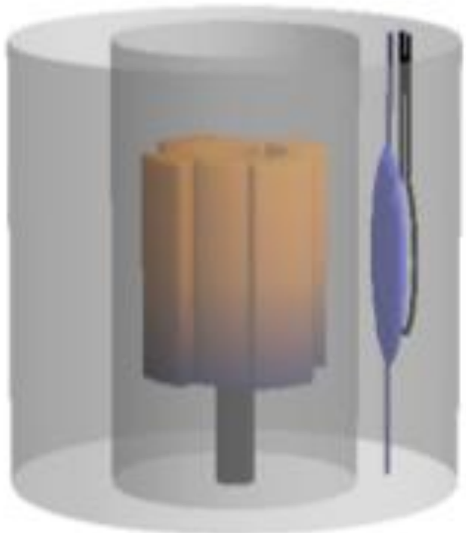

$$H_{\text{int}} = \frac{g_f m_f}{f_a} \vec{\nabla} a(x) \cdot \vec{\sigma}$$

the rotating mass on the left produces an oscillating axion field

the oscillating axion field is an effective magnetic field in an NMR experiment

$$\omega = \gamma_N B_0$$

Axion dark matter detection using an LC circuit

PS, D. Tanner and N. Sullivan, 2013

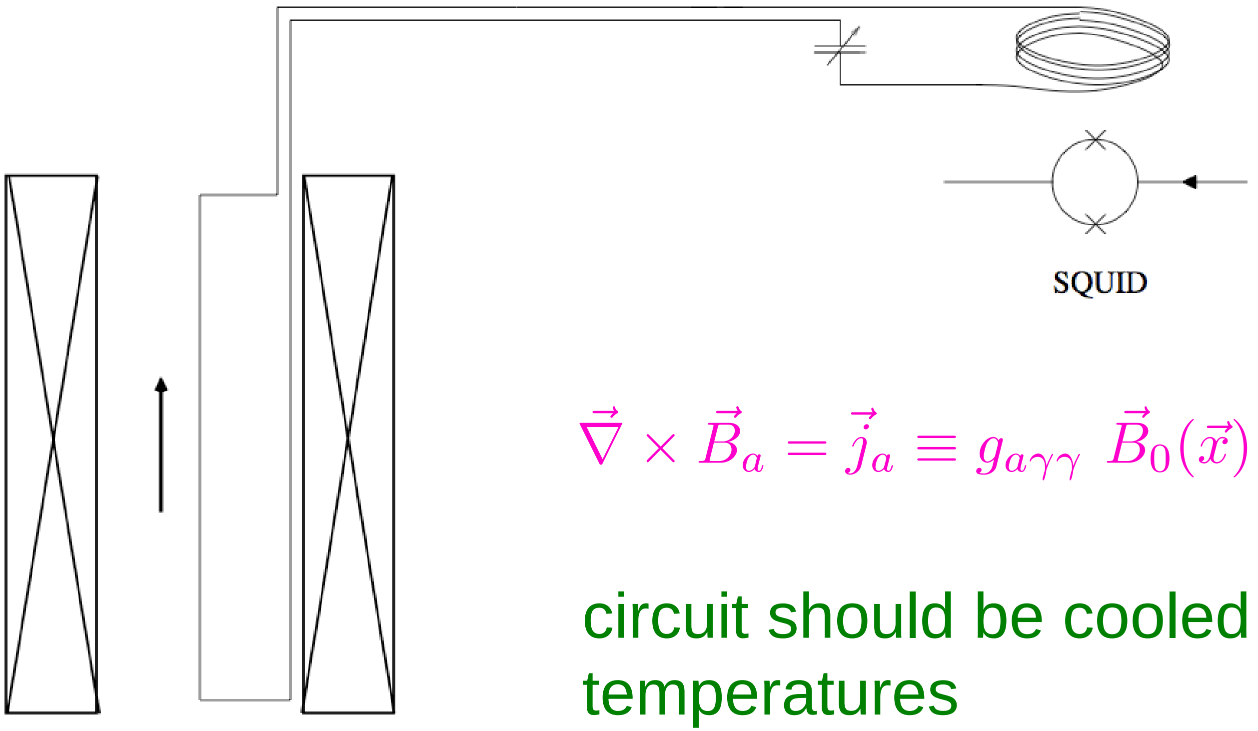

$$\vec{\nabla} \times \vec{B}_a = \vec{j}_a \equiv g_{a\gamma\gamma}\ \vec{B}_0(\vec{x})\ \partial_t a(\vec{x}, t)$$

circuit should be cooled to milli-Kelvin temperatures

ABRACADABRA, SLIC, DMRadio

Axion photon constraints

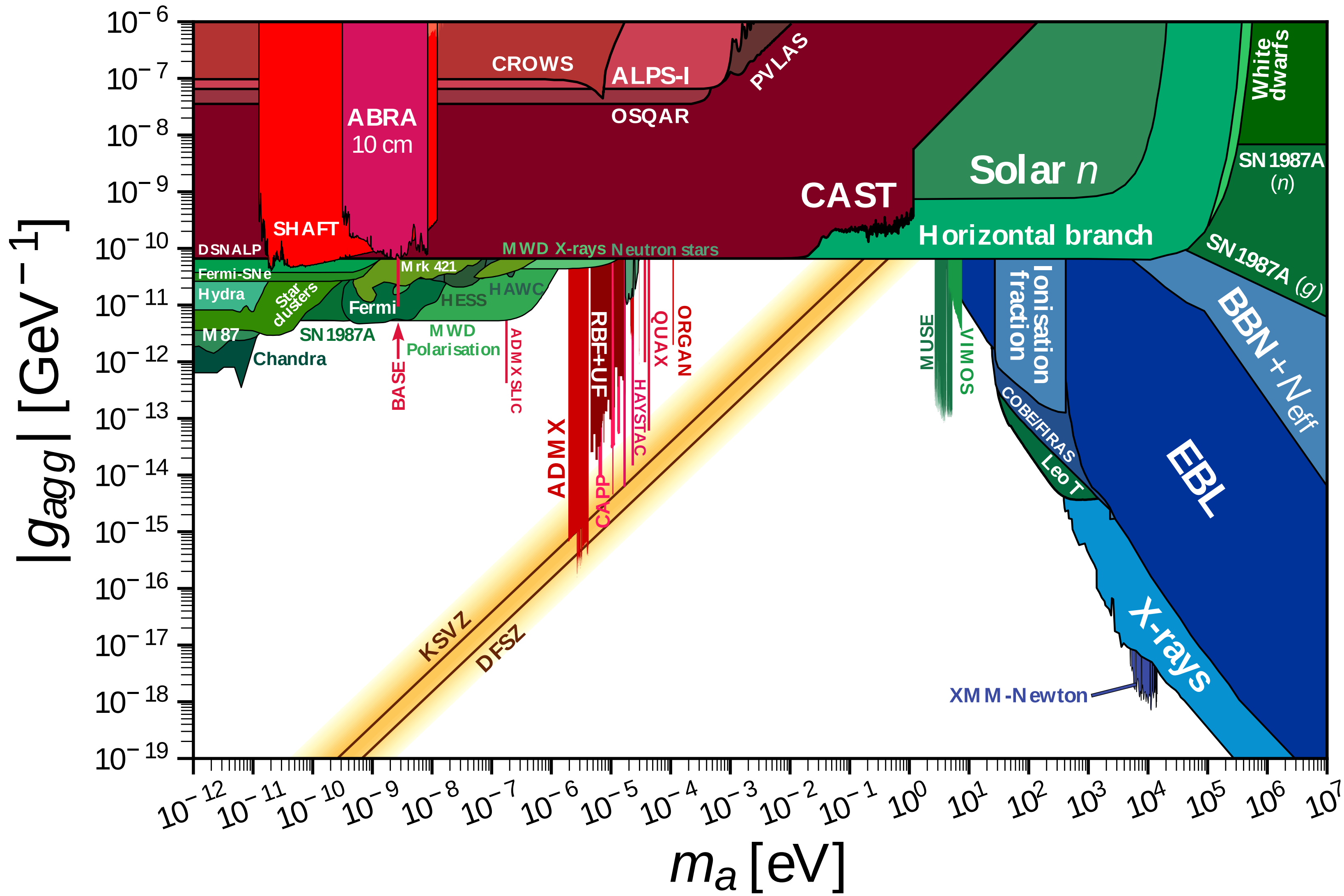

from https://cajohare.github.io/AxionLimits/

Stimulated axion decay

A. Arza
& PS, 2019

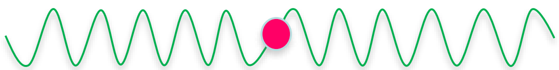

$$\Gamma(a \to 2\gamma) \sim \frac{1}{10^{51}\ \mathrm{sec}}$$

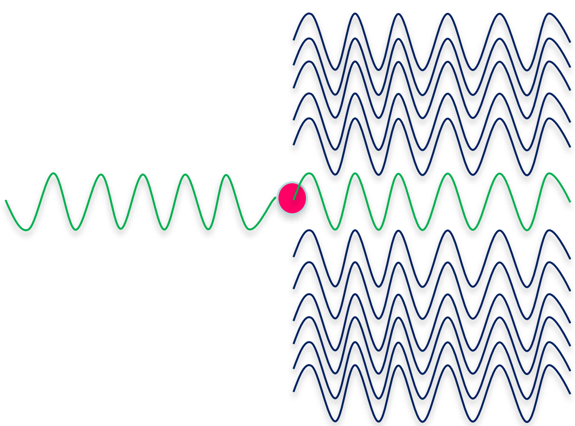

P_1 P_0

$$\omega = \frac{m_a}{2}$$

$$P_0 = \text{outgoing power}$$

$P_1 = \text{echo power}$

Conclusions

- Axions solve the strong CP problem
- A population of cold axions is naturally produced in the early universe which may be the dark matter today
- Axion dark matter is detectable